

# The Hele-Shaw injection problem for an extremely shear-thinning fluid

G. RICHARDSON<sup>1</sup> and J. R. KING<sup>2</sup>

<sup>1</sup>*Mathematical Sciences, University of Southampton, Southampton, SO17 1BJ, UK  
email: G.Richardson@soton.ac.uk*

<sup>2</sup>*School of Mathematical Sciences, University of Nottingham, Nottingham, NG7 2RD, UK  
email: John.King@nottingham.ac.uk*

(Received 25 December 2014; revised 30 June 2015; accepted 30 June 2015; first published online 23 July 2015)

We consider Hele-Shaw flows driven by injection of a highly shear-thinning power-law fluid (of exponent  $n$ ) in the absence of surface tension. We formulate the problem in terms of the streamfunction  $\psi$ , which satisfies the  $p$ -Laplacian equation  $\nabla \cdot (|\nabla\psi|^{p-2}\nabla\psi) = 0$  (with  $p = (n+1)/n$ ) and use the method of matched asymptotic expansions in the large  $n$  (extreme-shear-thinning) limit to find an approximate solution. The results show that significant flow occurs only in (I) segments of a (single) circle centred on the injection point, whose perimeters comprise the portion of free boundary closest to the injection point and (II) an exponentially small region around the injection point and (III) a transition region to the rest of the fluid: while the flow in the latter is exponentially slow it can be characterised in detail.

**Key words:** power law fluids, matched asymptotic expansions, free boundary problems,  $p$ -Laplace equation

## 1 Introduction

The problems of injection into and suction from a fluid region, with a moving boundary, in a Hele-Shaw cell has been the subject of a great deal of interest for over seventy years. The early work in this area arose from considering Darcy flow of groundwater (or oil) in a porous medium [18, 30]. In two dimensions this model, in its simplest guise, is mathematically equivalent to a Newtonian Hele-Shaw free boundary problem, consisting of Laplace's equation for pressure  $p$  and streamfunction  $\psi$  coupled to free boundary conditions. A variety of complex variable techniques (described in [20]) have been applied to such problems, much of the impetus of which arose from the results of Polubarinova-Kochina (e.g. [30]) whose work in the field is summarised in [28]. A notable feature of solutions to the zero-surface-tension (ZST) Newtonian Hele-Shaw problem is that, where fluid is injected, the solutions remain smooth but that, under suction, finite-time singularities in the free-boundary develop. This has resulted in a large literature on the possible regularisation of the ill-posed suction problem ranging from analytic approaches in the limit of vanishing surface tension [14, 21] to numerical ones that determine solutions to the suction problem with small, but finite, surface tension [12, 23]. Another remarkable feature of the ZST Newtonian Hele-Shaw problem is that it has an integrable structure with an infinite set of *moments* that evolve in an explicitly predictable manner [31].

In comparison to the Newtonian Hele-Shaw problem, flows of power-law fluids have received relatively little attention, despite the importance of shear-thinning fluids in injection moulding applications, for example. This may, in part, be attributed to the difficulty in dealing with the non-linear  $p$ -Laplace equations satisfied by the pressure and the streamfunction, in place of the linear ones, amenable to complex variable methods, that govern these quantities in the Newtonian case. Nevertheless progress has been made. Aronsson and Janfalk [6] have obtained similarity solutions describing flow in a corner, flow about a doublet and spiral flows. King [25] has investigated free boundary flows in the vicinity of the interface, focussing particularly on the local solution in proximity to a corner in the free boundary. Alexandrou and Entov [1] have investigated the ZST Saffman–Taylor problem for injection in a power-law fluid; they use a hodograph transformation to convert the non-linear free-boundary problem to a linear one on a fixed domain, which they tackle numerically in order to determine the shapes of the resulting Saffman–Taylor fingers for a variety of shear-thinning exponents. Power-law Saffman–Taylor problems have also been investigated by Amar and Poiré [8,9] and Richardson and King [32]. In the former, the weakly shear-thinning limit is investigated and, on the basis of numerical evidence, it is hypothesised that the selected finger width  $\lambda$  tends to zero as the surface tension coefficient reduces to zero; in contrast, in the Newtonian limit the selected finger width, in the ZST limit, is  $\lambda = 1/2$  (see [37] and references therein). In the latter, [32], the strongly shear-thinning limit of the ZST power-law Saffman–Taylor problem is investigated using asymptotic methods to show that finger shape tends to a semi-infinite strip. As noted by Aronsson [4] this limit is pertinent to the injection moulding of plastics – the limit in question is thus appealing not only because of its relative analytical tractability (and corresponding numerical difficulty, the ‘permeability’  $|\nabla p|^{n-1}$  potentially varying over many orders of magnitude) but also for its physical relevance. In the current work we instead focus on the asymptotic structure of the ZST moving-boundary problem that arises as a strongly shear-thinning power-law fluid is injected into a Hele-Shaw cell containing a blob of (this) fluid surrounded by air. Such extreme shear-thinning power-law Hele-Shaw flows are described by the large  $n$ -limit of elliptic PDEs for the streamfunction  $\psi$  and pressure  $p$

$$\nabla \cdot \left( \frac{\nabla \psi}{|\nabla \psi|^{1-1/n}} \right) = 0, \quad \text{and} \quad \nabla \cdot (|\nabla p|^{n-1} \nabla p) = 0, \quad (1.1)$$

which have been considered in a variety of other contexts (see, for example, [7]). The naive large  $n \rightarrow \infty$  limits to these elliptic equations are

$$\nabla \cdot \left( \frac{\nabla \psi}{|\nabla \psi|} \right) = 0, \quad \text{and} \quad |\nabla p| = 1, \quad (1.2)$$

respectively. The former equation (for the streamfunction) is parabolic and its solutions have the property that their level sets (the streamlines) are straight lines (indeed, the left-hand side is simply the mean curvature in a level-set formulation), while the latter is the eikonal equation (this equation appearing in geometric optics as well as describing the height of a critically-posed sandpile with fixed angle of repose). It is notable that these two equations can be mapped to each other and, indeed, that the level sets of  $\psi$  form

the rays of the hyperbolic eikonal equation: in keeping with the Hele-Shaw application we are concerned here with the two-dimensional case only. The degeneracy of the large  $n$ -limit is illustrated by the difference in type between the limit equations (1.2) and the original elliptic (for  $0 < n < \infty$ ) equations (1.1).

The ZST condition can be formulated as the following (equivalent) conditions on the moving boundary  $\partial\Omega$  between the power-law fluid and the air:

$$\left. \frac{\partial\psi}{\partial N} \right|_{\partial\Omega} = \nabla\psi \cdot N|_{\partial\Omega} = 0, \quad \text{and} \quad p|_{\partial\Omega} = 0, \quad (1.3)$$

where  $N$  is the unit normal to  $\partial\Omega$ . The former implies that the streamlines of the flow meet the moving boundary normally in the ZST case. As can be seen by tracking the rays of the eikonal equations from the source it is clear that the only solution to the limit equations (1.2) that describes flow from a single point source has the form

$$\psi = \frac{Q}{2\pi}\phi, \quad p = r, \quad (1.4)$$

where  $r$  and  $\phi$  are polar coordinates centred on the source and  $Q$  is the fluid flux emanating from the source. The ZST free boundary conditions imply that the free boundary is then a circle centred on the source, of form  $r = R(t)$  where, by conservation of fluid,  $R$  evolves according to

$$\frac{dR}{dt} = \frac{Q}{2\pi R}.$$

This can evidently be the limit solution to (1.2) only in the radially symmetric case, already implying that subtleties must of necessity arise in the limit process in more general domains, i.e. (1.2) cannot provide a uniformly valid description of the more general case. An approach based on solving the naive limit equation (1.2a) to the free-boundary problem, comprised of (1.1a) and (1.3a), provides a good description of the salient features of the large- $n$  injection problem and has been rigorously formulated by Aronsson [2] as a *distance model*. This can be loosely summarised as the moving boundary being divided into (i) arcs of circles centred on the injection point, moving with uniform velocity, and (ii) stationary sections that lie further from the injection point than the moving arcs (see Figure 1(b)). The flow has an essentially plastic nature being divided into ‘yielded’ regions bounded by the arcs formed by the moving boundary and the straight lines joining the extremities of those arcs to the injection point and ‘unyielded’ regions everywhere else. In this sense the flow mimics that of a Bingham plastic. Moreover, this picture has been verified experimentally by Piscotti *et al.* [29], who have favourably compared solutions to the distance model with injection moulding experiments in which polystyrene (a highly shear-thinning fluid) was injected into an industrial mould. Nevertheless, the injection problem is still worth investigating from the view point of formal asymptotics as there are a number of unresolved questions about the nature of the flow for finite, but large, values of  $n$ . These include, for example, how the transition occurs between the regions of ‘yielded’ flow lying behind the advancing sections of boundary and the ‘unyielded’ flow elsewhere, questions on the nature of the flow in the immediate vicinity of the injection point and on the magnitude and nature of the flow in the ‘unyielded’ regions. It is also

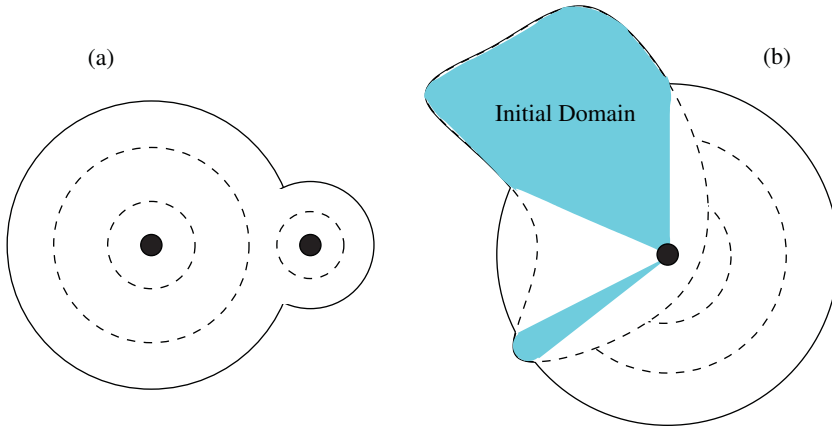


FIGURE 1. Injection (to leading-order) from (a) two points with no fluid initially present (and sources of unequal strength) and (b) from a single point into an initially fluid filled domain. Here dashed lines show previous positions of the fluid domain, while the solid one shows the present position, the shaded areas being associated with the unyielded regions.

envisaged that the asymptotic structure of the problem may provide insight into the suction problem in the limit of small surface tension. The current widespread interest in the  $p$ -Laplace equation provides additional, intrinsically mathematical, motivation for such studies. Before leaving the naive distance model we remark that it has also successfully been applied in an industrial setting in [4] and to squeeze-film problems by Aronsson and Evans [5] and Bergwall [10] but that the approach is not directly applicable to the problem of injection of a Saffman–Taylor finger (of any gas) into a channel filled with a strongly shear-thinning power-law fluid, as discussed in [32].

The asymptotic structure of extremely shear-thinning power-law fluids, not constrained in a Hele–Shaw cell, has been investigated by Brewster *et al.* [11] and Chapman *et al.* [13], who note that even very simple flows exhibit a rich asymptotic structure.

## 2 Problem formulation

The velocity of the fluid  $\mathbf{w}$  is given in terms of the pressure  $p$  by (working throughout in dimensionless terms)

$$\mathbf{w} = -|\nabla p|^{n-1} \nabla p. \quad (2.1)$$

Assuming incompressibility leads to

$$\nabla \cdot (|\nabla p|^{n-1} \nabla p) = 0. \quad (2.2)$$

Alternatively, the problem can be formulated in terms of the streamfunction  $\psi$  defined by

$$\mathbf{w} = \frac{\partial \psi}{\partial y} \mathbf{e}_x - \frac{\partial \psi}{\partial x} \mathbf{e}_y. \quad (2.3)$$

This leads to following ‘Cauchy–Riemann’ relations between  $p$  and  $\psi$

$$\frac{\partial p}{\partial x} = -\frac{1}{|\nabla\psi|^{1-1/n}} \frac{\partial \psi}{\partial y}, \quad \frac{\partial p}{\partial y} = \frac{1}{|\nabla\psi|^{1-1/n}} \frac{\partial \psi}{\partial x}, \tag{2.4}$$

(so that the streamlines and isobars are orthogonal) and hence to  $|\nabla\psi| = |\nabla p|^n$  and to

$$\nabla \cdot \left( \frac{\nabla\psi}{|\nabla\psi|^{1-1/n}} \right) = 0. \tag{2.5}$$

The Cartesian representation of (2.1) and (2.5) are given in Appendix A while some of the properties of the system (2.4) are discussed in Appendix B, with references to the relevant literature.

In the case of ZST the boundary conditions on the free boundary  $\partial\Omega_f$  (with outward normal  $\mathbf{N}$ ) are

$$p|_{\partial\Omega_f} = 0, \quad v_N = -|\nabla p|^{n-1} \frac{\partial p}{\partial N} \Big|_{\partial\Omega_f}, \tag{2.6}$$

where  $v_N$  is the normal velocity of the boundary. The zero pressure condition can equally be translated to a condition on the normal derivative of the streamfunction on the boundary so that the conditions on the streamfunction take the form

$$\frac{\partial \psi}{\partial N} \Big|_{\partial\Omega_f} = 0, \quad v_N = \frac{\partial \psi}{\partial s} \Big|_{\partial\Omega_f}, \tag{2.7}$$

where  $\partial/\partial s$  is the tangential derivative along the boundary taken in an anti-clockwise sense.

In the immediate vicinity of the injection point the leading-order flow is radially symmetric. Thus, where the injected flux is  $Q$ , the boundary conditions on the pressure and streamfunction at the injection point is

$$p \sim \hat{P}(t) - \left( \frac{Q}{2\pi} \right)^{1/n} \frac{r^{1-1/n}}{1-1/n} \quad \text{as } r \rightarrow 0, \tag{2.8}$$

$$\psi \sim \frac{Q\phi}{2\pi} \quad \text{as } r \rightarrow 0, \tag{2.9}$$

where  $r$  and  $\phi$  are plane-polar coordinates centred at the injection point,  $r$  measuring distance from this point and  $\phi$  the angle about it, in the standard fashion. As is usual, in such problems,  $\psi$  is multivalued resulting in the problem being formulated with a branch cut. Here, we shall take the branch cut along  $\phi = \pi$  (i.e. through the middle of region V as illustrated in Figure 2).

### 2.1 Formulation of the problem, in terms of pressure and streamfunction, in polar coordinates

Given that the streamlines in this problem all emanate from the injection point, at the origin, it proves helpful to formulate the problem in terms of radial polar coordinates

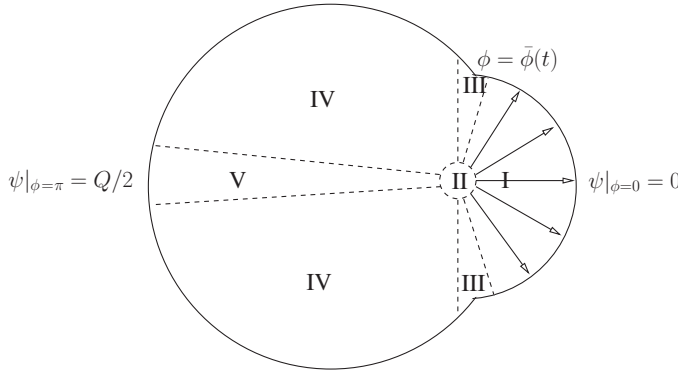


FIGURE 2. The asymptotic regions for injection into an off-centred circle.

centred at the injection point as described above. Defining the position of the free boundary by  $r = g(\phi, t)$  leads to the following pressure formulation of the problem (which we derive from (2.2), (2.6) and (2.8)):

$$\left(p_r^2 + \frac{1}{nr^2}p_\phi^2\right)p_{rr} + \frac{2}{r^2}\left(1 - \frac{1}{n}\right)p_r p_\phi p_{r\phi} + \frac{1}{r^2}\left(\frac{1}{r^2}p_\phi^2 + \frac{1}{n}p_r^2\right)p_{\phi\phi} + \frac{1}{nr}p_r^3 - \frac{1}{r^3}\left(1 - \frac{2}{n}\right)p_r p_\phi^2 = 0, \tag{2.10}$$

$$p \sim \hat{P}(t) - \left(\frac{Q}{2\pi}\right)^{1/n} \frac{r^{1-1/n}}{1 - 1/n} \text{ as } r \rightarrow 0, \tag{2.11}$$

$$p|_{r=g(\phi,t)} = 0, \quad \frac{\partial g}{\partial t} = \left(\frac{p_\phi g_\phi}{g^2} - p_r\right) \left(p_r^2 + \frac{p_\phi^2}{g^2}\right)^{(n-1)/2} \Big|_{r=g(\phi,t)}. \tag{2.12}$$

The equivalent streamfunction formulation, obtained from (2.5), (2.7) and (2.9), is

$$\left(\frac{1}{r^2}\psi_\phi^2 + \frac{1}{n}\psi_r^2\right)\psi_{rr} - \frac{2}{r^2}\left(1 - \frac{1}{n}\right)\psi_r\psi_\phi\psi_{r\phi} + \frac{1}{r^2}\left(\psi_r^2 + \frac{1}{nr^2}\psi_\phi^2\right)\psi_{\phi\phi} + \frac{1}{r}\psi_r^3 + \frac{1}{r^3}\left(2 - \frac{1}{n}\right)\psi_r\psi_\phi^2 = 0, \tag{2.13}$$

$$\psi \sim \frac{Q\phi}{2\pi} \text{ as } r \rightarrow 0, \tag{2.14}$$

$$g\psi_r - \frac{g_\phi}{g}\psi_\phi \Big|_{r=g(\phi,t)} = 0, \quad \frac{\partial g}{\partial t} = \frac{1}{g}(\psi_\phi + g_\phi\psi_r) \Big|_{r=g(\phi,t)}, \tag{2.15}$$

and is closed by specifying the initial shape of the blob in the form of an initial condition on the free boundary

$$g(\phi, 0) = h(\phi). \tag{2.16}$$

The radial ‘Cauchy–Riemann’ equations, analogous to (2.4), are

$$\frac{\partial p}{\partial r} = - \left( \left( \frac{\partial \psi}{\partial r} \right)^2 + \frac{1}{r^2} \left( \frac{\partial \psi}{\partial \phi} \right)^2 \right)^{-(1-1/n)/2} \frac{1}{r} \frac{\partial \psi}{\partial \phi}$$

$$\frac{1}{r} \frac{\partial p}{\partial \phi} = \left( \left( \frac{\partial \psi}{\partial r} \right)^2 + \frac{1}{r^2} \left( \frac{\partial \psi}{\partial \phi} \right)^2 \right)^{-(1-1/n)/2} \frac{\partial \psi}{\partial r}.$$

### 3 Asymptotic solution for $\psi$

In the following, we look for an asymptotic solution to the streamfunction formulation of the problem as formulated in (2.5), (2.7) and (2.9), or equivalently in (2.13)–(2.15), based on large exponent  $n$ . In order to accomplish this we will need to divide physical domain up into different regions, constructing leading-order asymptotic problems in each (in the sense of matched asymptotic expansions) and matching these together across their common boundaries. These regions are pictorially represented in Figure 2 for a typical example of an injection problem (which started from a circular region of fluid with an off centre injection point), but our analysis is equally applicable to any initial fluid domain. As described in the introduction we only expect the flows to be significant in the ‘yielded’ regions in the immediate vicinity of the injection point (region II) and in one (or more) segments of a circle (region I), centred on the injection point, comprising those portions of the free boundary lying closest to the injection point. It follows that this is the only part over which the free boundary advances appreciably. The other main region is an ‘unyielded’ one (region IV) that is bounded by the remaining portions of the free boundary; the free boundary in region IV lies further from the injection point than that portion bounding region I and here the flow is exponentially slow, so that the free boundary is to a good approximation stationary. Physical insight into the reasons for this follows from the observation that the shear-thinning nature of the fluid leads to one, or more, self-reinforcing regions of least resistance, the much higher viscosities elsewhere strongly suppressing flow. The remaining regions, III and V, depicted in Figure 2 serve respectively to match between the significant flows in region I and the exponentially small flows in region IV and between the parts of region IV on either side of a streamline joining the injection point to a point on the boundary whose distance from the injection point is a local maximum, respectively.

In order to aid the clarity of exposition we shall assume that the fluid domain is symmetric about the  $x$ -axis (that is, about  $\phi = 0$  and  $\phi = \pi$ ) and that the distance of the initial free boundary from the injection point  $r = g(\phi, 0)$  has only a single local minimum and a single local maximum. It follows from the symmetry that  $\phi = 0$  and  $\phi = \pi$  are streamlines so that, for a source of strength  $Q$  as on (2.14), the boundary conditions on the streamfunction to this symmetric problem are

$$\psi|_{\phi=0} = 0, \quad \text{and} \quad \psi|_{\phi=\pi} = Q/2. \tag{3.1}$$

Here, the symmetry of the problem obviates the need for explicitly introducing a branch cut. We claim that it is not particularly difficult to generalise the analysis to other cases

but note that where there are multiple local minima of  $g(\phi, 0)$  we should expect multiple yielded regions (analogous to region I and hence additional regions of type III) to appear as the evolution progresses.

### 3.1 Region I

#### 3.1.1 Preamble

Here, we shall look for a ‘yielded’ region of the flow that carries a significant portion of the fluid flux, emanating from the source, to the free boundary. Given that  $|\nabla\psi| = O(Q)$  throughout the region we expect the dominant balance in the streamfunction equation (2.5) to be provided by the naive limit (1.2a). As stated in Section 1 the level sets (streamlines) of (2.5) are straight lines and so the only solution to (2.5) capable of describing flow driven by a source is one in which the streamlines lie along radii of a circle centred on the source. The ZST free boundary condition (2.7a) then implies that the free boundary lies along an arc of this circle. We shall assume that region I comprises a growing segment of this circle lying, above the  $x$ -axis, in  $0 \leq \phi < \bar{\phi}(t)$  and, below it, in  $2\pi - \bar{\phi}(t) < \phi < 2\pi$ . As we noted in the introduction regions of ‘unyielded’ flow are associated with segments of free boundary lying further from the source than the segments of ‘yielded’ free boundary (such as that bounding region I). That the flow in these unyielded regions is exponentially small can be inferred from the pressure formulation of the problem, (2.1)–(2.2) and (2.6). It can be readily be deduced that  $|\nabla p|$  is smaller in the unyielded region than in the yielded one because the distance between the maximum pressure point (at the injection site) and the zero pressure contour (the free boundary) is greater in the unyielded region than in the yielded one where the free boundary is closest to the injection point. It follows that in the large  $n$  limit the fluid velocity (as defined by (2.1)) in the unyielded region is exponentially small in comparison to that in the yielded region. As a consequence the free boundary to region I swallows neighbouring portions of the (almost) stationary ‘unyielded’ free boundary, as time progresses, causing  $\bar{\phi}(t)$  to increase with time, a point which we return to in Section 4.

In order to complete the description of this region of ‘yielded’ flow we look for an asymptotic solution to (2.13)–(2.15) of the form

$$\psi^{(I)} = \psi_0^{(I)}(r, \phi) + \frac{1}{n} \psi_1^{(I)}(r, \phi) + \dots, \quad g^{(I)} = g_0^{(I)}(t) + \dots.$$

This yields the following leading-order problem:

$$\frac{1}{r^2} \left( \frac{\partial \psi_0^{(I)}}{\partial \phi} \right)^2 \frac{\partial^2 \psi_0^{(I)}}{\partial r^2} - \frac{2}{r^2} \frac{\partial \psi_0^{(I)}}{\partial r} \frac{\partial \psi_0^{(I)}}{\partial \phi} \frac{\partial^2 \psi_0^{(I)}}{\partial r \partial \phi} + \frac{1}{r^2} \left( \frac{\partial \psi_0^{(I)}}{\partial r} \right)^2 \frac{\partial^2 \psi_0^{(I)}}{\partial \phi^2} + \frac{1}{r} \left( \frac{\partial \psi_0^{(I)}}{\partial r} \right)^3 + \frac{2}{r^3} \frac{\partial \psi_0^{(I)}}{\partial r} \left( \frac{\partial \psi_0^{(I)}}{\partial \phi} \right)^2 = 0, \tag{3.2}$$

$$\left. \frac{\partial \psi_0^{(I)}}{\partial r} \right|_{r=g_0^{(I)}(t)} = 0, \quad g_0^{(I)} \frac{\partial g_0^{(I)}}{\partial t} = \left. \frac{\partial \psi_0^{(I)}}{\partial \phi} \right|_{r=g_0^{(I)}(t)} \tag{3.3}$$

Here, (3.2) is the limit equation (1.2) formulated in radial coordinates. The level sets of its solution are (as already stated) straight lines. Because,  $g_0^{(I)}$  is independent of  $\phi$  and the streamlines are straight lines emanating from the origin the required solution is

$$\psi_0^{(I)} = K(t)\phi, \quad g_0^{(I)2} = 2 \int_0^t K(t')dt',$$

where the function  $K(t)$  can be determined by matching to region II for the flow about the injection point at the origin. However, it can also be obtained more immediately by conservation of fluid since, to leading-order, the entire injected flux enters region I; this leads us to deduce that  $K(t) = Q/(2\bar{\phi}(t))$  and

$$\psi_0^{(I)} = \frac{Q}{2\bar{\phi}(t)}\phi \quad \text{in } 0 \leq \phi < \bar{\phi}(t), \quad g_0^{(I)2} = \int_0^t \frac{Q}{\bar{\phi}(t')}dt'. \tag{3.4}$$

The corresponding leading-order solution for the pressure, satisfies the eikonal equation, is zero on the free boundary and is given by  $p_0^{(I)} = g_0^{(I)}(t) - r$ .

### 3.1.2 Evolution of interface between yielded and unyielded regions

The initial condition (2.16) implies the initial shape of the blob is given by  $r = h(\phi)$  and, as stated previously, we assume  $h(\phi)$  to be monotonically increasing in  $\phi$  in  $0 < \phi < \pi$ . The division between the yielded and unyielded regions of the free-boundary thus occurs at  $r = h(\bar{\phi}(t)) = g_0^{(I)}(t)$  and  $\phi = \bar{\phi}(t)$ . It follows that the radial velocity of this point is equal to that of the yielded free boundary (region I), which from (3.4) is  $Q/(2\bar{\phi}(t)g_0^{(I)}(t))$  and hence

$$h'(\bar{\phi}(t))\bar{\phi}'(t) = \frac{Q}{2\bar{\phi}(t)h(\bar{\phi}(t))}; \tag{3.5}$$

this ordinary differential equation is what determines  $\bar{\phi}(t)$ .

## 3.2 Region II

Here, we look for a small (indeed exponentially small) region of ‘yielded’ flow about the injection point in which the flow adjusts from its radially symmetric configuration, in the immediate vicinity of the origin, to the wedge shaped flow in region I. We start by introducing a stretched radial coordinate via the substitution

$$r = \exp(-n\rho),$$

in terms of which the problem (2.13)–(2.14) becomes

$$\left(\frac{1}{n}\psi_\phi^2 + \frac{1}{n^4}\psi_\rho^2\right)\psi_{\rho\rho} - \frac{2}{n}\left(1 - \frac{1}{n}\right)\psi_\rho\psi_\phi\psi_{\rho\phi} + \left(\psi_\phi^2 + \frac{1}{n}\psi_\rho^2\right)\psi_{\phi\phi} - \left(1 - \frac{1}{n}\right)\left(\psi_\rho\psi_\phi^2 + \frac{1}{n^2}\psi_\rho^3\right) = 0, \tag{3.6}$$

$$\psi \sim \frac{Q\phi}{2\pi} \quad \text{as } \rho \rightarrow \infty. \tag{3.7}$$

Expanding  $\psi$  in the above, in the form

$$\psi^{(II)} = \psi_0^{(II)} + \frac{1}{n}\psi_1^{(II)} + \dots,$$

and matching to the leading-order solution for the streamfunction in region I (3.4) leads to a closed problem for  $\psi_0^{(II)}$  in the form of an IBVP for the heat equation

$$\frac{\partial \psi_0^{(II)}}{\partial \rho} = \frac{\partial \psi_0^{(II)}}{\partial \phi^2} \quad \text{for } 0 < \rho < \infty \quad \text{for } 0 \leq \phi < \pi, \tag{3.8}$$

$$\psi_0^{(II)}|_{\rho=0} = \begin{cases} \frac{Q\phi}{2\bar{\phi}(t)} & \text{in } 0 \leq \phi < \bar{\phi}(t), \\ \frac{Q}{2} & \text{in } \bar{\phi}(t) \leq \phi \leq \pi, \end{cases} \tag{3.9}$$

$$\psi_0^{(II)}|_{\phi=0} = 0 \quad \text{and} \quad \psi_0^{(II)}|_{\phi=\pi} = \frac{Q}{2}, \tag{3.10}$$

$$\psi_0^{(II)} \sim \frac{Q\phi}{2\pi} \quad \text{as } \rho \rightarrow \infty. \tag{3.11}$$

It is notable that ‘causality’ in (3.8) (i.e. the direction of increasing  $\rho$ ) involves moving into, rather than out of, the source, which is perhaps counterintuitive. The solution to (3.8)–(3.11) reads

$$\psi_0^{(II)} = \frac{Q}{2\pi} \left( \phi + \sum_{k=1}^{\infty} \left( \frac{2 \sin(k\bar{\phi}(t))}{k^2 \bar{\phi}(t)} \right) \sin(k\phi) \exp(-k^2 \rho) \right), \tag{3.12}$$

and is illustrated in Figure 3. The small  $\rho$  behaviour to (3.8)–(3.9) is given by

$$\psi_0^{(II)} \sim \frac{Q}{2} \left( 1 - \frac{\rho^{1/2}}{\bar{\phi}(t)} F \left( \frac{\phi - \bar{\phi}(t)}{2\rho^{1/2}} \right) \right) \quad \text{as } \rho \rightarrow 0, \tag{3.13}$$

$$\text{where } F(\eta) = \frac{1}{\sqrt{\pi}} e^{-\eta^2} + \eta (\text{erf}(\eta) - 1). \tag{3.14}$$

Rewriting this behaviour, for  $\phi > \bar{\phi}(t)$ , in terms of the region IV variables ( $r = \exp(-n\rho)$  and  $\phi$ ), and exploiting the large  $\eta$  asymptotic behaviour of  $F(\eta)$ , gives

$$\psi_0^{(II)} \sim \frac{Q}{2} - \frac{Q(\log(1/r))^{3/2}}{n^{3/2} \sqrt{\pi} \bar{\phi}(t) (\phi - \bar{\phi}(t))^2} \exp \left( -n \frac{(\phi - \bar{\phi}(t))^2}{4 \log(1/r)} \right) \quad \text{as } \rho \rightarrow 0 \quad \phi > \bar{\phi}(t), \tag{3.15}$$

which serves as a matching condition, as  $r \rightarrow 0$ , on the leading-order region IV problem. Notably (3.13), the small  $\rho$  behaviour of  $\psi_0^{(II)}$ , exhibits a boundary layer about  $\phi = \bar{\phi}(t)$  and on re-expressing it in terms of the region III variables (defined such that  $\zeta = n^{1/2}(\phi - \bar{\phi})$  and  $r = \exp(-n\rho)$ ) yields

$$\psi_0^{(II)} \sim \frac{Q}{2} \left( 1 - \frac{(\log(1/r))^{1/2}}{n^{1/2} \bar{\phi}} F \left( \frac{\zeta}{2(\log(1/r))^{1/2}} \right) \right) \quad \text{as } \rho \rightarrow 0 \quad \text{with } \zeta = O(1), \tag{3.16}$$

(where  $F(\cdot)$  is defined in (3.14)), corresponding and serving as the required initial data there.

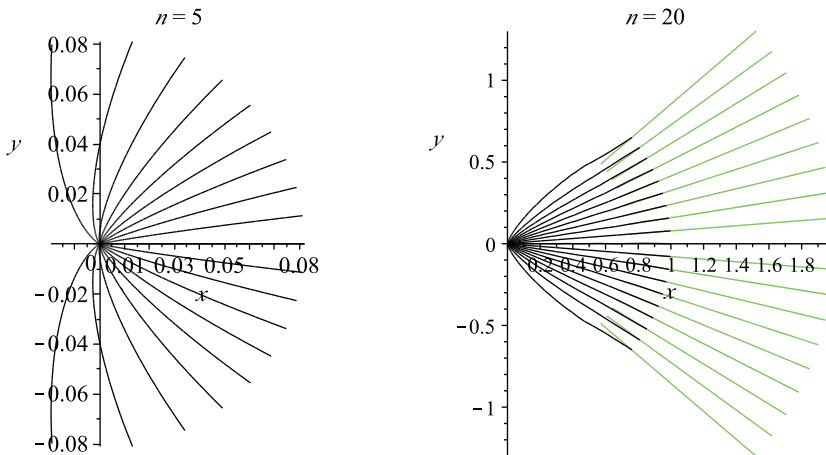


FIGURE 3. The leading-order solution for the streamfunction  $\psi^{(II)}$  in region II (plotted in physical space) with  $\bar{\phi} = \pi/4$ . The first panel shows a moderately large value of the exponent,  $n = 5$ , and illustrates the flow close to the injection point while the second shows a very large value of the exponent,  $n = 20$ , and illustrates the matching between the flow and that in region I (streamlines in region I are shown by light coloured curves). The exponentially stretched nature of solution in this region means that it is hard to illustrate both of these features for a single value of  $n$ .

The behaviour for  $p$  in this region is, to leading-order, radially symmetric, being given by  $p \sim \hat{P}(t) - r$  (where  $\hat{P}(t) = g_0^{(I)}(t)$  to match to the solution for the pressure in region I). It is therefore seen that the problem is much more conveniently expressed in terms of the streamfunction, whose leading-order solution encapsulates information about the flow, in a way that the leading-order pressure does not.

### 3.3 Region IV

In this region the flow is exponentially small and here we make the following (Liouville–Green or JWKB) solution ansatz in  $\bar{\phi} < \phi < \pi$

$$\psi^{(IV)} = \frac{Q}{2} - \frac{1}{n^{3/2}} \exp(-n\beta(x, y, t)), \tag{3.17}$$

where  $\beta$  is an  $O(1)$  function of space and time. Substituting this into (2.5) leads to the following equation for  $\beta$

$$\nabla \cdot \left( \frac{\nabla\beta}{|\nabla\beta|^{1-1/n}} \right) = |\nabla\beta|^{1+1/n}. \tag{3.18}$$

Expanding  $\beta$  in the obvious fashion

$$\beta = \beta_0 + \dots, \tag{3.19}$$

as  $n \rightarrow \infty$  yields the following parabolic PDE for  $\beta_0$ :

$$\nabla \cdot \left( \frac{\nabla\beta_0}{|\nabla\beta_0|} \right) = |\nabla\beta_0|. \tag{3.20}$$

This limit problem is also discussed in Appendix B. Equation (3.20) for  $\beta_0$  couples to free boundary conditions (obtained from substituting (3.17) into (2.7))

$$\left. \frac{\partial \beta_0}{\partial N} \right|_{\partial \Omega_f} = 0, \quad \log(v_N) = -n\beta_0|_{\partial \Omega_f}. \tag{3.21}$$

It is apparent that the free-boundary in this region is to a very good approximation stationary, so that

$$g^{(III)} \sim h(\phi),$$

where  $r = h(\phi)$  is the initial position of the free boundary; indeed,  $g$  is perturbed from the initial data by only an exponentially small amount.

### 3.3.1 Matching to region II

Here, we match  $\psi^{(IV)}$  as  $r \rightarrow 0$  to the leading-order solution in region II via its small  $\rho$  behaviour which is re-expressed in the appropriate range of  $\phi$ , and in terms of region IV variables, in (3.15). A matching condition on  $\beta_0$  is then obtained by comparing (3.15) to the ansatz (3.17), in which  $\beta$  is expanded as in (3.19); it is

$$\beta_0 \sim \frac{(\phi - \bar{\phi}(t))^2}{4 \log(\frac{1}{r})} \quad \text{as } r \rightarrow 0. \tag{3.22}$$

### 3.3.2 Formulation of the problem as flow by inverse curvature

Interfacial dynamics formulations of the type

$$q_N = G(\kappa), \tag{3.23}$$

where  $q_N$  is the normal velocity of a plane curve of curvature  $\kappa$  have been the subject of a great deal of attention, for example [26, 33, 35]. Expressing the curve in level set form  $t = \omega(\mathbf{x})$  implies that

$$q_N = \frac{1}{|\nabla \omega|} \quad \text{and} \quad \kappa = -\nabla \cdot \left( \frac{\nabla \omega}{|\nabla \omega|} \right),$$

so that

$$|\nabla \omega| G \left( \nabla \cdot \left( \frac{\nabla \omega}{|\nabla \omega|} \right) \right) = -1. \tag{3.24}$$

Identifying  $\beta_0$  with  $\omega$  we see that (3.24) corresponds to (3.20) in the special case  $G(\kappa) = -1/\kappa$  of flow by the reciprocal of curvature, that is to the motion of a two-dimensional curve evolving with the velocity law

$$q_N = -\frac{1}{\kappa}. \tag{3.25}$$

This result has been remarked upon by Moser [27] who noted that (3.20) is the level set formulation of (3.25). Formulating the problem in terms of dependent variable  $Y$  and independent variables  $x$  and  $\beta_0$ , where  $(x, y) = (x, Y(x, \beta_0))$ , so that  $\beta_0$  plays the role of a time variable, and gives (on matching to region I) the initial condition

$$Y|_{\beta_0=0} = x \tan(\bar{\phi}). \tag{3.26}$$

The boundary condition is obtained from the consideration of (3.21),

$$(1, Y_x) \cdot \mathbf{N}|_{\partial\Omega_f} = 0, \quad Y(0, \beta_0) = 0. \tag{3.27}$$

and is equivalent to requiring that the level sets of  $\beta_0$  meet the boundary of the fluid filled region,  $\partial\Omega_f$ , normally.

We remark further that it is possible to linearise (3.25) to the heat equation (cf. [36]). This can be accomplished, for example, by transforming (3.25) into an equation for the curvature  $\kappa$  in terms of the independent variables  $\theta$  and  $t$  where  $\theta$  is the angle made by the curve with the  $x$ -axis. As detailed in [19], for example, curvature flows of the form (3.23), are mapped, under this transformation, to the PDE

$$\frac{\partial\kappa}{\partial\tau} = \kappa^2 \left( \frac{\partial^2 G(\kappa)}{\partial\theta^2} + G(\kappa) \right).$$

Thus, in this particular instance (with  $G = -1/\kappa$ ) we obtain

$$\frac{\partial\kappa}{\partial\tau} = -\kappa^2 \left( \frac{\partial^2}{\partial\theta^2} \left( \frac{1}{\kappa} \right) + \frac{1}{\kappa} \right),$$

which on substituting for the radius of curvature  $R = 1/\kappa$  transforms into a heat equation with a linear source

$$\frac{\partial R}{\partial t} = \frac{\partial^2 R}{\partial\theta^2} + R. \tag{3.28}$$

Unfortunately, the boundary conditions on the free boundary make further analytic progress problematic in the current case.

We next discuss the boundary condition on (3.20) at  $y = 0$ . For (2.5) we have  $\psi = Q/2$  along this streamline, but nevertheless it is not possible to prescribe  $\beta_0 \rightarrow +\infty$  as  $y \rightarrow 0$  and a straight streamline (i.e. level set of  $\beta$ ) would move with infinite speed in the framework of (3.25). Thus the situation in Figure 4(a) is not possible and the scenario is as in Figure 4(b) (associated in (3.25) with level sets of  $\beta_0$  advancing as slowly as they can along  $y = 0$ , i.e. with satisfying the condition the condition  $\beta_0 \rightarrow +\infty$  there as ‘closely’ as they are able, given that  $\beta_0$  corresponds to the time variable in (3.25)).

We now substantiate these assertions via a local analysis of (3.20), i.e. of

$$\left( \frac{\partial\beta_0}{\partial y} \right)^2 \frac{\partial^2\beta_0}{\partial x^2} - 2 \frac{\partial\beta_0}{\partial x} \frac{\partial\beta_0}{\partial y} \frac{\partial^2\beta_0}{\partial x\partial y} + \left( \frac{\partial\beta_0}{\partial x} \right)^2 \frac{\partial^2\beta_0}{\partial y^2} = \left( \left( \frac{\partial\beta_0}{\partial x} \right)^2 + \left( \frac{\partial\beta_0}{\partial y} \right)^2 \right)^2. \tag{3.29}$$

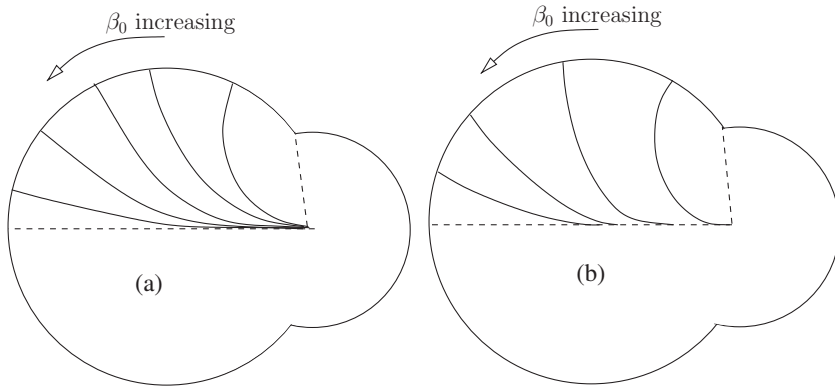


FIGURE 4. (a) Inadmissible level sets of  $\beta_0$  for (3.20), even though they (corresponding as they do to streamlines) all emerge from the source. (b) Schematic of the actual level sets; note by (3.25) that each necessarily has negative  $\kappa$  throughout its length – thus the geometric interpretation of (3.20) in terms of (3.25) provides insight into the streamline structure even in the absence of numerical solution.

For solutions having a Taylor expansion in  $y$ ,

$$\beta_0(x, y) \sim \alpha_0(x) + \alpha_1(x)y + \frac{1}{2}\alpha_2(x)y^2 \quad \text{as } y \rightarrow 0^+. \tag{3.30}$$

( $d\alpha_0/dx < 0$  must hold throughout what follows) a single relationship

$$\alpha_1^2 \frac{d^2\alpha_0}{dx^2} - 2\alpha_1 \frac{d\alpha_0}{dx} \frac{d\alpha_1}{dx} + \left(\frac{d\alpha_0}{dx}\right)^2 \alpha_2 = \left(\left(\frac{d\alpha_0}{dx}\right)^2 + \alpha_1^2\right)^2, \tag{3.31}$$

between the three coefficients in (3.30) ensues, so that a single condition on  $\beta_0$  and  $\partial\beta_0/\partial y$  on  $y = 0$  should be prescribed to obtain a correctly specified problem; i.e. a contact angle condition on  $\partial\beta_0/\partial y$  could be imposed, for example. However, the local behaviour (3.30) (having finite contact angle) does not allow matching into region V and the required condition is instead

$$\frac{\partial\beta_0}{\partial y} \rightarrow -\infty \quad \text{as } y \rightarrow 0^+. \tag{3.32}$$

We remark in passing from (3.31) that symmetric solutions,  $\alpha_1 \equiv 0$ , have

$$\alpha_2 = \left(\frac{d\alpha_0}{dx}\right)^2 > 0,$$

in (3.30), as in effect required by (3.25). It readily follows from (3.29) that the cuspidal behaviour indicated in Figure 4(b) is associated with a local expansion

$$\beta_0(x, y) \sim \alpha_0(x) - \gamma(x)y^{2/3} \quad \text{as } y \rightarrow 0^+, \tag{3.33}$$

wherein

$$\gamma(x) = \frac{(3\alpha'_0(x))^{2/3}}{2}. \tag{3.34}$$

Thus (3.20) is to be solved subject to (3.32), implying local behaviour (3.33)–(3.34). The problem is almost in a form suitable for numerical solution; that the limit problem (3.20) is degenerate (in that unlike (3.18) with  $0 < n < \infty$ , it is not elliptic) suggest that a level set approach would be an appropriate one. Level sets are required to meet the free boundary (which is prescribed as its initial location) orthogonally and the centre line  $\phi = \pi$  tangentially; the contact points with both need to be tracked as part of the solution, but perhaps the most delicate issue numerically is associated with the initial data – setting  $y = x \tan \phi$  at  $\beta_0 = 0$ , as implied by matching into region I, implies that  $\kappa = 0$  at  $\beta_0 = 0$  and hence a small-time singularity associated with the transition into region III.

### 3.4 Region III

This region serves as the transition between regions I and IV and is the most challenging of all (indeed we shall not fully resolve it here). We recall that in region I the free boundary  $r = g_0^{(I)}(t)$  moves with velocity determined by (3.4b) while in region IV it is to a good approximation stationary so that, to leading-order, it lies along its initial position  $r = h(\phi)$ . In order to match across the narrow region III lying about the edge of region I along  $\phi = \bar{\phi}(t)$  continuity of the free boundary enforces (as noted above)

$$g_0^{(I)}(t) = h(\bar{\phi}(t)).$$

In this region we rescale about  $\phi = \bar{\phi}(t)$ , by writing  $\zeta = n^{1/2}(\phi - \bar{\phi}(t))$ , so that time and azimuthal derivatives transform via

$$\frac{\partial}{\partial t} \rightarrow \frac{\partial}{\partial t} - n^{1/2} \bar{\phi}'(t) \frac{\partial}{\partial \zeta} \quad \text{and} \quad \frac{\partial}{\partial \phi} = n^{1/2} \frac{\partial}{\partial \zeta}.$$

Under this rescaling the conditions on the free-boundary (2.15) transform to

$$g^2 \frac{\partial \psi}{\partial r} - n \frac{\partial g}{\partial \zeta} \frac{\partial \psi}{\partial \zeta} \Big|_{r=g(\zeta,t)} = 0, \quad g \frac{\partial g}{\partial t} - n^{1/2} \bar{\phi}'(t) g \frac{\partial g}{\partial \zeta} = n^{1/2} \left( \frac{\partial \psi}{\partial \zeta} + \frac{\partial g}{\partial \zeta} \frac{\partial \psi}{\partial r} \right) \Big|_{r=g(\zeta,t)}. \tag{3.35}$$

Motivated by the form of the solution in regions I, II and IV, to which the solution in region III must match, and by the fact that the leading-order free boundary has a jump in derivative between region I and IV we expand the dependent variables in this region as follows:

$$\psi = \frac{Q}{2} + \frac{1}{n^{1/2}} \psi_0^{(III)}(r, \zeta) + \dots, \tag{3.36}$$

$$g^{(III)} = h(\bar{\phi}(t)) + \frac{1}{n^{1/2}} g_1^{(III)}(\zeta, t) + \dots. \tag{3.37}$$

One possible scenario is as follows (we note again that we do not fully characterise region III here: indeed it seems likely that at least one further region is present associated with

the transition between cases (i) and (ii) in (3.40)–(3.41)). Substitution of (3.37) into (3.35) gives, at leading-order, the following relations

$$\left. \frac{\partial g_1^{(III)}}{\partial \zeta} \frac{\partial \psi_0^{(III)}}{\partial \zeta} \right|_{r=h(\bar{\phi})} = 0. \tag{3.38}$$

$$h(\bar{\phi})\bar{\phi}'(t) \left( h'(\bar{\phi}) - \frac{\partial g_1^{(III)}}{\partial \zeta} \right) \Big|_{r=h(\bar{\phi})} = \left. \frac{\partial \psi_0^{(III)}}{\partial \zeta} \right|_{r=h(\bar{\phi})}. \tag{3.39}$$

In order that (3.38) be satisfied either  $g_{1,\zeta}^{(III)} = 0$  or  $\psi_{0,\zeta}^{(III)}|_{r=h(\bar{\phi})} = 0$ . In the former case (3.39) then implies  $\frac{\partial \psi_0^{(III)}}{\partial \zeta}|_{r=h(\bar{\phi})} = h(\bar{\phi})h'(\bar{\phi})\bar{\phi}'(t)$  while in the latter it implies  $g_{1,\zeta}^{(III)} = h'(\bar{\phi}(t))$ . We thus obtain a linear complementarity condition on  $\psi_0^{(III)}$  which states

$$\text{either (i) } \left. \frac{\partial \psi_0^{(III)}}{\partial \zeta} \right|_{r=h(\bar{\phi})} = 0 \quad \text{or (ii) } \left. \frac{\partial \psi_0^{(III)}}{\partial \zeta} \right|_{r=h(\bar{\phi})} = \frac{Q}{2\bar{\phi}(t)}, \tag{3.40}$$

where we use the fact that  $h'(\bar{\phi})\bar{\phi}'(t)$  is given by (3.5). The corresponding conditions on the free boundary are

$$\text{either (i) } \frac{\partial g_1^{(III)}}{\partial \zeta} = h'(\bar{\phi}(t)) \quad \text{or (ii) } \frac{\partial g_1^{(III)}}{\partial \zeta} = 0, \tag{3.41}$$

and can be interpreted as stating that either (i) the free boundary is, to the first two orders, given by its initial configuration ( $g \sim h(\bar{\phi}(t) + \zeta/n^{1/2})$ ) or (ii) it lies along a circular arc (centred on the source at the origin).

Substitution of the expansions (3.36) and (3.37) into (2.13)–(2.14), and matching to the leading-order solutions in regions I, II and IV, results in the following problem for  $\psi_0^{(III)}$ :

$$\begin{aligned} & \left( \frac{\partial \psi_0^{(III)}}{\partial \zeta} \right)^2 \frac{\partial^2 \psi_0^{(III)}}{\partial r^2} - 2 \frac{\partial \psi_0^{(III)}}{\partial r} \frac{\partial \psi_0^{(III)}}{\partial \zeta} \frac{\partial \psi_0^{(III)}}{\partial r \partial \zeta} \\ & + \left( \left( \frac{\partial \psi_0^{(III)}}{\partial r} \right)^2 + \frac{1}{r^2} \left( \frac{\partial \psi_0^{(III)}}{\partial \zeta} \right)^2 \right) \frac{\partial^2 \psi_0^{(III)}}{\partial \zeta^2} + \frac{2}{r} \frac{\partial \psi_0^{(III)}}{\partial r} \left( \frac{\partial \psi_0^{(III)}}{\partial \zeta} \right)^2 = 0, \end{aligned} \tag{3.42}$$

$$\psi_0^{(III)} \rightarrow 0 \quad \text{as } \zeta \rightarrow +\infty, \tag{3.43}$$

$$\psi_0^{(III)} \sim \frac{Q\zeta}{2\bar{\phi}(t)} \quad \text{as } \zeta \rightarrow -\infty, \tag{3.44}$$

$$\psi_0^{(III)} \sim -\frac{Q}{2} \frac{(\log(\frac{1}{r}))^{1/2}}{\bar{\phi}(t)} F \left( \frac{\zeta}{2(\log(\frac{1}{r}))^{1/2}} \right) \quad \text{as } r \rightarrow 0, \tag{3.45}$$

$$\left. \frac{\partial \psi_0^{(III)}}{\partial \zeta} \right|_{r=h(\bar{\phi})} = 0 \quad \text{for } \zeta < 0, \quad \left. \frac{\partial \psi_0^{(III)}}{\partial \zeta} \right|_{r=h(\bar{\phi})} = \frac{Q}{2\bar{\phi}(t)} \quad \text{for } \zeta > 0, \tag{3.46}$$

(where the function  $F(\cdot)$  is defined in (3.14)) together with an equation for the correction

to the free boundary position in  $\zeta > 0$

$$\frac{\partial g_2^{(III)}}{\partial \zeta} = \frac{h'(\bar{\phi}(t))^2 + h(\bar{\phi}(t))^2}{h(\bar{\phi}(t))h'(\bar{\phi}(t))\bar{\phi}'(t)} \frac{\partial \psi_0^{(III)}}{\partial r} \Big|_{r=h(\bar{\phi}(t))}.$$

It is notable that (3.42) is a second order elliptic<sup>1</sup> PDE and that coupling it to the boundary data (3.43)–(3.46) leads to a problem that might reasonably be expected to be well-posed and thus susceptible to numerical solution. We remark further that the free boundary determined in region III appears non-smooth on this scale, containing a jump in the derivative with respect to  $\zeta$  at  $\zeta = 0$ ; further analysis of this is required, however.

### 3.4.1 Transformation to stretched Cartesian coordinates

The change to stretched Cartesian coordinates  $\mathfrak{x} = -h(\bar{\phi})r\zeta$  and  $\eta = h(\bar{\phi})r$  and a rescaling of the dependent variable  $\psi_0^{(III)} = (Q/(2\bar{\phi}(t))\Psi$  maps the problem from polars, with stretched radial variable, to stretched Cartesian coordinates. With this change of coordinates transformation (3.42)–(3.46) transforms to the problem

$$\frac{\partial^2 \Psi}{\partial \mathfrak{x}^2} \left( \left( \frac{\partial \Psi}{\partial \eta} \right)^2 + \left( \frac{\partial \Psi}{\partial \mathfrak{x}} \right)^2 \right) - 2 \frac{\partial \Psi}{\partial \mathfrak{x}} \frac{\partial \Psi}{\partial \eta} \frac{\partial^2 \Psi}{\partial \mathfrak{x} \partial \eta} + \left( \frac{\partial \Psi}{\partial \mathfrak{x}} \right)^2 \frac{\partial^2 \Psi}{\partial \eta^2} = 0, \tag{3.47}$$

$$\frac{\partial \Psi}{\partial \mathfrak{x}} \Big|_{\eta=1} = -1 \quad \mathfrak{x} > 0, \quad \frac{\partial \Psi}{\partial \mathfrak{x}} \Big|_{\eta=1} = 0 \quad \mathfrak{x} < 0, \tag{3.48}$$

$$\Psi \Big|_{\eta=0, \mathfrak{x} < 0} = 0, \tag{3.49}$$

$$\Psi \sim -\frac{\mathfrak{x}}{\eta} \quad \text{as} \quad \frac{\mathfrak{x}}{\eta} \rightarrow +\infty, \tag{3.50}$$

$$\Psi \rightarrow 0 \quad \text{as} \quad \frac{\mathfrak{x}}{\eta} \rightarrow -\infty, \tag{3.51}$$

$$\frac{\partial \Psi}{\partial \mathfrak{x}} \rightarrow -\infty \quad \text{as} \quad (\mathfrak{x}, \eta) \rightarrow (0, 0), \tag{3.52}$$

$$\frac{\partial \Psi}{\partial \eta} \rightarrow -\infty \quad \text{as} \quad (\mathfrak{x}, \eta) \rightarrow (0, 0) \quad \text{with} \quad \mathfrak{x} < 0. \tag{3.53}$$

We remark that the partial differential equation (3.47), satisfied by  $\Psi$ , also occurs when analysing the streamfunction (for such an extreme shear-thinning power-law fluid) about the leading edge of a Saffman–Taylor finger as the flow slowly adjusts to the width of the cell [32]. If as in that case, we take a Legendre transform of the problem, namely map to the Legendre plane via

$$\begin{aligned} \hat{\mathfrak{x}} &= \frac{\partial \Psi}{\partial \mathfrak{x}}, & \hat{\eta} &= \frac{\partial \Psi}{\partial \eta}, & \hat{\Psi} &= \mathfrak{x} \frac{\partial \Psi}{\partial \mathfrak{x}} + \eta \frac{\partial \Psi}{\partial \eta} - \Psi, \\ \mathfrak{x} &= \frac{\partial \Psi}{\partial \hat{\mathfrak{x}}}, & \eta &= \frac{\partial \Psi}{\partial \hat{\eta}}, & \Psi &= \hat{\mathfrak{x}} \frac{\partial \Psi}{\partial \hat{\mathfrak{x}}} + \hat{\eta} \frac{\partial \Psi}{\partial \hat{\eta}} - \hat{\Psi}. \end{aligned} \tag{3.54}$$

<sup>1</sup> This feature is significant: the other limit problems discussed thus far have been degenerate.

and transform derivatives in the usual fashion (see, for example, (B 5)–(B 8)), the resulting problem takes the form

$$(\hat{x}^2 + \hat{\eta}^2) \frac{\partial^2 \hat{\Psi}}{\partial \hat{x}^2} + 2\hat{x}\hat{\eta} \frac{\partial^2 \hat{\Psi}}{\partial \hat{x} \partial \hat{\eta}} + \hat{x}^2 \frac{\partial^2 \hat{\Psi}}{\partial \hat{\eta}^2} = 0, \tag{3.55}$$

$$\frac{\partial \hat{\Psi}}{\partial \hat{\eta}} = 1 \quad \text{on} \quad \hat{x} = -1 \quad \text{with} \quad \hat{\eta} > s(-1), \tag{3.56}$$

$$\frac{\partial \hat{\Psi}}{\partial \hat{\eta}} = 1 \quad \text{and} \quad \frac{\partial \hat{\Psi}}{\partial \hat{\eta}} = 0 \quad \text{on} \quad \hat{\eta} = s(\hat{x}), \tag{3.57}$$

$$\frac{\partial \hat{\Psi}}{\partial \hat{\eta}} = 1 \quad \text{on} \quad \hat{x} = 0 \quad \text{with} \quad 0 < \hat{\eta} < s(0), \tag{3.58}$$

$$\frac{\partial \hat{\Psi}}{\partial \hat{\eta}} = 0 \quad \text{on} \quad \hat{x} = 0 \quad \text{with} \quad \hat{\eta} < 0, \tag{3.59}$$

$$\hat{\Psi} \sim -\frac{\hat{\eta}}{\hat{x}} \quad \text{as} \quad \hat{\eta} \rightarrow \infty \quad \text{for} \quad \hat{x} < -1, \tag{3.60}$$

$$\hat{\Psi} \rightarrow 0 \quad \text{as} \quad \hat{x} \rightarrow -\infty, \tag{3.61}$$

$$\hat{\Psi} \rightarrow 0 \quad \text{as} \quad \hat{\eta} \rightarrow -\infty, \tag{3.62}$$

where the position of the free boundary  $\hat{\eta} = s(\hat{x})$  needs to be determined as part of the solution. Here, (3.55) is associated with (3.47), (3.56)–(3.58) with (3.48), (3.59) with (3.50), (3.60) with (3.51), (3.61) with (3.52), and (3.62) with (3.53). The boundary conditions for this problem are illustrated in Figure 5.

### 3.5 Region V

Rescaling  $y$  in (2.5) about the dividing streamline  $\psi = Q/2$  (lying along  $y = 0, x < 0$ ) via

$$y = \frac{Y}{n^{3/2}}, \tag{3.63}$$

leads to the following equation for the streamfunction:

$$\left( \psi_Y^2 + \frac{1}{n^4} \psi_x^2 \right) \psi_{xx} - 2 \left( 1 - \frac{1}{n} \right) \psi_x \psi_Y \psi_{xY} + (\psi_x^2 + n^2 \psi_Y^2) \psi_{YY} = 0. \tag{3.64}$$

Then, in order to match into (3.33), the revised expansion for  $\psi$  takes the form

$$\psi \sim \frac{Q}{2} - \frac{1}{n^{3/2}} \exp(-n\alpha_0(x)) \left( \Theta_0 + \frac{1}{n} \Theta_1 + \dots \right), \tag{3.65}$$

whereby the dominant balance in (3.64) is

$$\alpha_0'^2 (\Theta_0^2 \Theta_{0,Y} - \Theta_0 \Theta_{0,Y}^2) + \Theta_{0,Y}^2 \Theta_{0,Y} = 0.$$

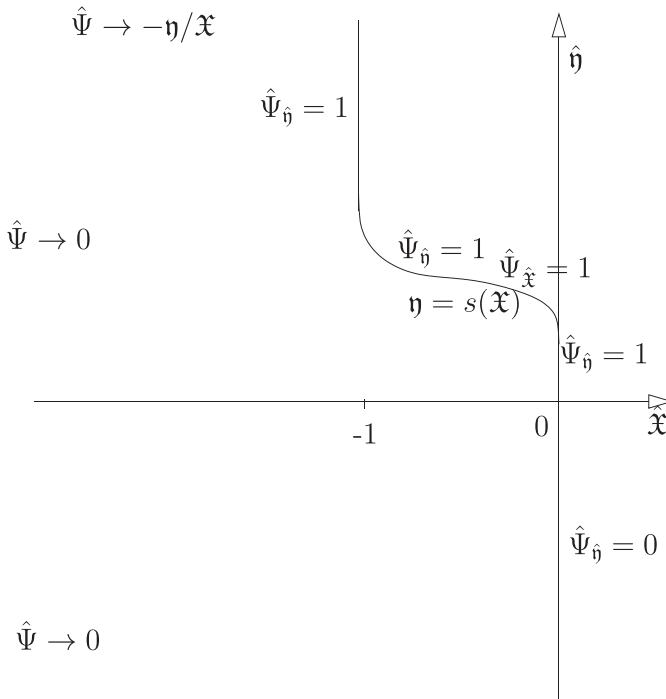


FIGURE 5. The boundary conditions to the Legendre transformed problem in region III.

By dividing this equation by  $\Theta_{0,Y}^3$  we can express this as an exact derivative

$$\frac{\partial}{\partial Y} \left( \log \left( \frac{\partial \Theta_0}{\partial Y} \right) - \frac{1}{2} \left( \frac{\alpha'_0(x)\Theta_0}{\partial \Theta_0 / \partial Y} \right)^2 \right) = 0, \tag{3.66}$$

with boundary condition (arising from the condition  $\psi|_{Y=0} = Q/2$ )

$$\Theta_0 = 0, \quad \text{on } Y = 0. \tag{3.67}$$

The symmetry of the problem implies that  $\Theta_0(x, Y)$  is odd in  $Y$  (being positive for  $Y > 0$ ) and in addition this, and the scaling (3.65), imply that  $\Theta_{0,Y}$  is positive and even in  $Y$ .

Integrating (3.66) gives

$$\log \left( \frac{1}{A_1(x)} \frac{\partial \Theta_0}{\partial Y} \right) - \frac{1}{2} \left( \frac{\alpha'_0(x)\Theta_0}{\partial \Theta_0 / \partial Y} \right)^2 = 0, \tag{3.68}$$

where

$$A_1(x) = \left. \frac{\partial \Theta_0}{\partial Y} \right|_{Y=0}.$$

Determining  $A_1(x)$  would require a higher-order expansion in region IV ( $A_1(x)$  corresponds to an  $O(1/n)$  contribution to  $\alpha_0$  in (3.65)) but its form is fortunately irrelevant here.

Recalling that  $\alpha'_0(x) < 0$  and setting

$$\Theta_0 = \frac{A_1(x)}{|\alpha'_0(x)|} \Omega(|\alpha'_0(x)|Y),$$

implies that  $\Omega(\mathfrak{z})$  satisfies

$$\left(\frac{d\Omega}{d\mathfrak{z}}\right)^2 \log\left(\frac{d\Omega}{d\mathfrak{z}}\right) = \frac{1}{2}\Omega^2 \quad \text{and} \quad \frac{d\Omega}{d\mathfrak{z}}\Big|_{\mathfrak{z}=0} = 0. \tag{3.69}$$

This can be solved in parametric form by introducing  $A = d\Omega/d\mathfrak{z}$  and, perversely, differentiating (3.69) with respect to  $\mathfrak{z}$  so that

$$\frac{d^2\Omega}{d\mathfrak{z}^2} = \frac{\Omega}{2\log\left(\frac{d\Omega}{d\mathfrak{z}}\right) + 1},$$

and then eliminating  $\Omega$  using (3.69), via

$$\Omega = \begin{cases} 2^{1/2} \frac{d\Omega}{d\mathfrak{z}} \log^{1/2}\left(\frac{d\Omega}{d\mathfrak{z}}\right) & \text{in } \mathfrak{z} > 0 \\ -2^{1/2} \frac{d\Omega}{d\mathfrak{z}} \log^{1/2}\left(\frac{d\Omega}{d\mathfrak{z}}\right) & \text{in } \mathfrak{z} < 0 \end{cases},$$

Then, since  $A = 1$  on  $\mathfrak{z} = 0$ , we obtain

$$\frac{dA}{d\mathfrak{z}} = \text{sign}(\mathfrak{z}) \frac{2^{1/2} A \log^{1/2} A}{2\log A + 1},$$

which can be integrated to obtain the solution in parametric form (in  $\mathfrak{z} > 0$ )

$$\Omega = 2^{1/2} A \log^{1/2}(A) \quad \text{and} \quad \frac{4}{3} \log^{3/2} A + 2 \log^{1/2} A = 2^{1/2} \mathfrak{z} \quad \text{in } \mathfrak{z} > 0. \tag{3.70}$$

The solution in  $\mathfrak{z} < 0$  can be obtained by noting  $\Omega$  is odd in  $\mathfrak{z}$  (and positive in  $\mathfrak{z} > 0$ ) while  $A$  is positive and even in  $\mathfrak{z}$ . Moreover, (3.70) can be solved explicitly by writing  $A = \exp(2f^2(\mathfrak{z}))$  so that

$$\Omega = 2f(\mathfrak{z}) \exp(2f^2(\mathfrak{z})) \quad \text{and} \quad 8f^3(\mathfrak{z}) + 6f(\mathfrak{z}) = 3\mathfrak{z} \quad \text{in } \mathfrak{z} > 0.$$

The cubic for  $f$  can be solved in the standard fashion, the only root with the required property  $f > 0$  being

$$f(\mathfrak{z}) = \frac{1}{4} \left( \frac{16}{(9\mathfrak{z}^2 + 4)^{1/2} - 3\mathfrak{z}} \right)^{1/3} - \left( \frac{(9\mathfrak{z}^2 + 4)^{1/2} - 3\mathfrak{z}}{16} \right)^{1/3}, \tag{3.71}$$

with the corresponding solutions for  $\Omega$  and  $A$  being

$$\Omega(\mathfrak{z}) = 2f(\mathfrak{z}) \exp(2f^2(\mathfrak{z})) \quad \text{and} \quad A = \exp(2f^2(\mathfrak{z})) \quad \text{in} \quad \mathfrak{z} > 0. \tag{3.72}$$

We note in particular that

$$\log \Omega \sim \frac{(3\mathfrak{z})^{2/3}}{2} \quad \text{as} \quad \mathfrak{z} \rightarrow +\infty, \tag{3.73}$$

and thus matches successfully with (3.33)–(3.34).

The streamlines in this interior layer are thus very closely bunched, but escape from it according to the behaviour (3.33)–(3.34), in keeping with the pressure gradient driving the (exponentially slow) flow to the free boundary. The above analysis sheds some light on the singular nature of the Aronsson solution for  $n = +\infty$  discussed in Section 5 of Evans & Yu [17].

Finally in this context, we note that for non-symmetric domains the location of region V is itself determined by a free-boundary problem, whereby the continuity conditions

$$[\beta_0]_{-}^{+} = 0, \quad \left. \frac{\partial \beta_0}{\partial v} \right|_{+} = -\infty, \quad \left. \frac{\partial \beta_0}{\partial v} \right|_{-} = +\infty,$$

are imposed on the unknown free boundary corresponding to the streamline  $\psi = Q/2$ , where  $\partial/\partial v$  is the normal derivative to the free boundary in the ‘+’ direction. Equation (3.66) (with  $x$  now denoting the tangential variable) remains the dominant balance and, particularly given the linearisability of (3.18) (as described in Appendix B), such free-boundary problems may well be worth pursuing in their own right, including in terms of the co-dimension two free-boundary problem (cf. [22]) associated with where the dividing streamline meets the free boundary (e.g. how, if at all, this relates to the point within the fluid domain furthest from the source).

### 4 Discussion

In this work, we have applied the methods of formal matched asymptotics to investigate the structure of the Hele-Shaw injection problem for a power-law fluid in the limit of extreme shear-thinning (i.e. with large exponent  $n$ ) and in the absence of surface tension. To leading-order the free-boundary of the fluid region is divided into moving segments, consisting of circular arcs (of equal radii of curvature) centred on the injection point, and almost stationary segments that lie further from the injection point than the moving arcs. These results are associated with a plastic type flow that can be approximated by a division into ‘yielded’ regions (region I and region II, in our terminology) and ‘unyielded’ regions (region IV). The former are associated with the flow behind moving segments of the free-boundary and about the injection point. Our results for the streamfunction  $\psi$  and the position  $r = g(\phi, t)$  of the free boundary are summarised below for the three most

important regions

region I Main yielded region  $-\bar{\phi}(t) < \phi < \bar{\phi}(t)$

$$\psi \sim \frac{Q}{2\bar{\phi}(t)}\phi, \quad g(\phi, t) \sim \sqrt{\int_0^t \frac{Q}{\bar{\phi}(t')} dt'}$$

region II About injection point as  $r \rightarrow 0$

$$\psi \sim \frac{Q}{2\pi} \left( \phi + \sum_{k=1}^{\infty} \left( \frac{2 \sin(k\bar{\phi}(t))}{k^2 \bar{\phi}(t)} \right) \sin(k\phi) \exp \left( -\frac{k^2}{n} \ln \left( \frac{1}{r} \right) \right) \right),$$

region IV Unyielded region  $\bar{\phi}(t) < \phi < \pi$

$$\psi \sim \frac{Q}{2} - \frac{1}{n^{3/2}} e^{-n\beta}, \quad g(\phi, t) \sim g(\phi, 0),$$

$$\text{where } \nabla \cdot \left( \frac{\nabla \beta}{|\nabla \beta|} \right) \sim |\nabla \beta|.$$

Important aspects of these results for the limit  $n \rightarrow +\infty$  have previously been rigorously demonstrated by Aronsson [2] in the limit  $n \rightarrow +\infty$ . However, other than in region I, the latter approach leaves the details of the flow unresolved. The contribution of the current work include the elucidation of the asymptotic structure of the flow for large, but finite,  $n$ , demonstrating, for example, how the flow emerging from the injection point (in region II) adjusts to that in the yielded region (region I). As such it is a first step in understanding problems such as the (ill-posed) suction problem and the non-zero-surface-tension problem that do not seem well-suited to the approach adopted in [2] but that should, nevertheless, be amenable to matched asymptotics. In the ZST suction case, it is plausible that the only initial domains from which all the fluid can be extracted (without a free boundary singularity forming) are circles centred on the sink. Implicit in the above analysis of the injection case is that circular free boundaries are extremely stable in the very shear-thinning limit and hence, by time reversal, highly unstable for suction flows, highlighting the scope for, and interest of, the asymptotic analysis of the corresponding limit.

Other aspects of the analysis worth noting are the following. Exponential asymptotics central to the region IV (while region II is exponentially small) – by capturing these, the exponentially slow motion of the free boundary in the unyielded region can be precisely characterised. Such features suggest that the highly shear-thinning limit will be very challenging numerically, reinforcing the important complementary role played by the asymptotic analysis (related issues can be expected to arise also in the highly shear-thickening limit  $n \rightarrow 0$ , which is the dual to the current one in a sense noted in Appendix B). The subproblems derived here for each of the regions should be much more readily tractable numerically than the original problem though, given the degeneracy of many of the limit problems, the numerical approaches best suited to them may differ from those most appropriate to the original (elliptic) problem. We remark also that the asymptotic structure observed in the injection problem, treated here, is rather different to that of the equivalent Saffman–Taylor problem for large  $n$  power-law fluids considered

in [32]. Although, as for the injection problem, the latter has two significant regions, a yielded one (in which the flow is appreciable) and an unyielded one (in which the flow is exponentially slow), the problem is quite distinct from that examined here. In particular the yielded region, in front of the advancing Saffman–Taylor finger, adjusts slowly to the width cell and the corresponding streamfunction satisfies an elliptic problem, to leading order, rather than the (trivial) parabolic one satisfied by that in region I (of the injection problem).

We conclude by noting the rather diverse mathematical ingredients of the analysis needed for the resolution of the current problem. Alongside tracking exponentially small terms, we have appealed both to linearising transformations and interfacial dynamics formulations. Free boundaries, in addition to the physical one, arise in the limit cases, namely the locations of regions III and IV (the analysis shows the former to be trivial in the sense that is given by a straight-line ray, but the latter leads, in the unsymmetric case, to a non-trivial and perhaps novel free boundary formulation). Finally, the approaches developed here may prove fruitful in treating various other aspects of the  $p$ -Laplace equation and its applications.

**Appendix A The equations for pressure and streamfunction in Cartesian coordinates**

The problem for the pressure, (2.2) and (2.6), can be formulated in terms of Cartesian coordinates  $x$  and  $y$  as

$$\left(p_x^2 + \frac{1}{n}p_y^2\right)p_{xx} + 2\left(1 - \frac{1}{n}\right)p_xp_y p_{xy} + \left(p_y^2 + \frac{1}{n}p_x^2\right)p_{yy} = 0. \tag{A 1}$$

The equivalent formulation for the streamfunction, derived from (2.5) and (2.7), is

$$\left(\psi_y^2 + \frac{1}{n}\psi_x^2\right)\psi_{xx} - 2\left(1 - \frac{1}{n}\right)\psi_x\psi_y\psi_{xy} + \left(\psi_x^2 + \frac{1}{n}\psi_y^2\right)\psi_{yy} = 0. \tag{A 2}$$

**Appendix B Inverse curvature flow and the infinity Laplacian**

We collect here results relevant to the analysis of region IV, though some broader context concerning the  $p$ -Laplace equation for general  $n$  is also recorded.

The system (2.4) implies the pair of relations (1.1) and emphasises the duality between cases involving the exponents  $n$  and  $1/n$  in (and restricted to) the two-dimensional case. The situations in the limit cases  $n \rightarrow 0^+$  and  $n \rightarrow +\infty$  has a subtlety, however (cf. [16]): naively setting  $n = +\infty$  in the first of (1.1) leads to the degenerate case (1.2) (i.e. the 1-Laplacian) with

$$\frac{\partial p}{\partial x} = -\frac{1}{|\nabla\psi|} \frac{\partial\psi}{\partial y}, \quad \frac{\partial p}{\partial y} = \frac{1}{|\nabla\psi|} \frac{\partial\psi}{\partial x}, \tag{B 1}$$

but setting  $\psi = \exp(-n\beta)$  before taking the limit instead gives

$$\frac{\partial p}{\partial x} = e^{-\beta} \frac{1}{|\nabla\beta|} \frac{\partial\beta}{\partial y}, \quad \frac{\partial p}{\partial y} = -e^{-\beta} \frac{1}{|\nabla\beta|} \frac{\partial\beta}{\partial x}, \tag{B 2}$$

which on cross-differentiating to eliminate  $p$  leads to

$$\nabla \cdot \left( e^{-\beta} \frac{\nabla\beta}{|\nabla\beta|} \right) = 0 \quad \text{or, equivalently,} \quad \nabla \cdot \left( \frac{\nabla\beta}{|\nabla\beta|} \right) = |\nabla\beta|; \tag{B 3}$$

the former retains the divergence form while the latter coincides with a level-set representation of flow by inverse curvature (see above). Conversely  $\beta$  may be eliminated by observing that  $|\nabla p| = e^{-\beta}$ , denoting  $\mu = e^{-\beta}$  and re-expressing (B 2) in the form

$$\frac{1}{|\nabla p|} \frac{\partial p}{\partial x} = - \frac{1}{|\nabla\mu|} \frac{\partial\mu}{\partial y} \quad \frac{1}{|\nabla p|} \frac{\partial p}{\partial y} = \frac{1}{|\nabla\mu|} \frac{\partial\mu}{\partial x}.$$

It follows that  $\nabla\mu \cdot \nabla p = 0$  which, on substituting  $\mu = |\nabla p|$  yields the (two-dimensional)  $\infty$ -Laplace equation

$$\nabla p \cdot \nabla |\nabla p| = 0. \tag{B 4}$$

This is therefore the dual (in the above sense) to (B 3), rather than to the 1-Laplace equation. The study of this equation has been pioneered by Aronsson (see [3] and references therein). If  $|\nabla p| = \text{constant}$ , as in region I, (B 4) is automatically satisfied, but the converse need not be true, as in region IV above. We refer to [15] and [17] and for other references and recent results. We now proceed to note a number of reformulations that follow from (B 1)–(B 4).

**B.1 Legendre transformation of (B 4), the  $\infty$ -Laplace equation.**

The Legendre transformation

$$\mathcal{X} = \frac{\partial p}{\partial x}, \quad \mathcal{Y} = \frac{\partial p}{\partial y}, \quad \mathcal{P} = x \frac{\partial p}{\partial x} + y \frac{\partial p}{\partial y} - p, \tag{B 5}$$

transforms partial derivatives via

$$\frac{\partial}{\partial \mathcal{X}} = \frac{1}{J} \left( p_{yy} \frac{\partial}{\partial x} - p_{xy} \frac{\partial}{\partial y} \right), \quad \frac{\partial}{\partial \mathcal{Y}} = \frac{1}{J} \left( p_{xx} \frac{\partial}{\partial y} - p_{xy} \frac{\partial}{\partial x} \right) \tag{B 6}$$

where  $J = (p_{xx}p_{yy} - p_{xy}^2)$ .

By taking the partial derivatives of  $\mathcal{P}$  (as defined in (B 5)) with respect to  $\mathcal{X}$  and  $\mathcal{Y}$  we obtain the inverse transformation

$$x = \frac{\partial \mathcal{P}}{\partial \mathcal{X}}, \quad y = \frac{\partial \mathcal{P}}{\partial \mathcal{Y}}, \quad p = \mathcal{X} \frac{\partial \mathcal{P}}{\partial \mathcal{X}} + \mathcal{Y} \frac{\partial \mathcal{P}}{\partial \mathcal{Y}} - \mathcal{P}, \tag{B 7}$$

which transforms partial derivatives via

$$\frac{\partial}{\partial x} = \frac{1}{\mathcal{J}} \left( \mathcal{P}_{yy} \frac{\partial}{\partial \mathcal{X}} - \mathcal{P}_{xy} \frac{\partial}{\partial \mathcal{Y}} \right), \quad \frac{\partial}{\partial y} = \frac{1}{\mathcal{J}} \left( \mathcal{P}_{xx} \frac{\partial}{\partial \mathcal{Y}} - \mathcal{P}_{xy} \frac{\partial}{\partial \mathcal{X}} \right) \tag{B 8}$$

where  $\mathcal{J} = (\mathcal{P}_{xx}\mathcal{P}_{yy} - \mathcal{P}_{xy}^2) = \frac{1}{J}$ .

Following [3] we express (B 4) in the form  $\mathcal{X}(\partial/\partial x)(\sqrt{\mathcal{X}^2 + \mathcal{Y}^2}) + \mathcal{Y}(\partial/\partial y)(\sqrt{\mathcal{X}^2 + \mathcal{Y}^2}) = 0$  and transform the derivatives in this expression via (B 8) to obtain the Legendre transformation of the  $\infty$ -Laplace equation

$$\mathcal{X}^2 \mathcal{P}_{\mathcal{Y}\mathcal{Y}} - 2\mathcal{X}\mathcal{Y} \mathcal{P}_{\mathcal{X}\mathcal{Y}} + \mathcal{Y}^2 \mathcal{P}_{\mathcal{X}\mathcal{X}} = 0.$$

This can be more concisely expressed in terms of the polar coordinates

$$\mathcal{X} = \mathcal{R} \cos \Phi, \quad \mathcal{Y} = \mathcal{R} \sin \Phi, \tag{B 9}$$

as

$$\mathcal{R} \frac{\partial \mathcal{P}}{\partial \mathcal{R}} + \frac{\partial^2 \mathcal{P}}{\partial \Phi^2} = 0, \tag{B 10}$$

(again see [3]). In terms of these polar coordinates  $p$ , as defined in (B 9), can be expressed as

$$p = \mathcal{R}^2 \frac{\partial}{\partial \mathcal{R}} \left( \frac{\mathcal{P}}{\mathcal{R}} \right). \tag{B 11}$$

Dividing (B 10) by  $\mathcal{R}$  and then differentiating with respect to  $\mathcal{R}$  yields (on using (B 11)) the PDE for  $p$  in terms of the radial Legendre coordinates

$$\mathcal{R} \frac{\partial p}{\partial \mathcal{R}} + \frac{\partial^2 p}{\partial \Phi^2} = 0. \tag{B 12}$$

On recalling that  $|\nabla p| = e^{-\beta}$  in the limit  $n \rightarrow +\infty$ , we note that  $\beta$  can be expressed in terms of the Legendre coordinates as  $\beta = -\log R$ . Substitution of  $R$  for  $\beta$  in (B 10)–(B 12) then yields

$$\frac{\partial p}{\partial \beta} = \frac{\partial^2 p}{\partial \Phi^2}, \quad \frac{\partial \mathcal{P}}{\partial \beta} = \frac{\partial^2 \mathcal{P}}{\partial \Phi^2}, \quad p = -\mathcal{P} - \frac{\partial \mathcal{P}}{\partial \beta}, \tag{B 13}$$

i.e. the heat equation with  $\beta$  acting as the time-like variable.

In contrast to (2.5), equations (B 3) cannot directly be linearised by a Legendre transformation and it is worth noting how the associated limit then proceeds. The usual such transformation for (2.5) takes the form

$$\hat{\Psi} = x \frac{\partial \psi}{\partial x} + y \frac{\partial \psi}{\partial y} - \psi, \quad \hat{X} = \frac{\partial \psi}{\partial x}, \quad \hat{Y} = \frac{\partial \psi}{\partial y},$$

with inverse

$$\psi = \hat{X} \frac{\partial \hat{\Psi}}{\partial \hat{X}} + \hat{Y} \frac{\partial \hat{\Psi}}{\partial \hat{Y}} - \hat{\Psi}, \quad x = \frac{\partial \hat{\Psi}}{\partial \hat{X}}, \quad y = \frac{\partial \hat{\Psi}}{\partial \hat{Y}}. \tag{B 14}$$

On denoting  $\hat{R} = (\hat{X}^2 + \hat{Y}^2)^{1/2}$  and defining  $\hat{\Phi}$  so that  $\hat{X} = \hat{R} \cos \hat{\Phi}$  and  $\hat{Y} = \hat{R} \sin \hat{\Phi}$  we obtain (from the ‘Cauchy–Riemann’ equations (2.4)) the relations  $\hat{R} = \mathcal{R}^n$  and  $\hat{\Phi} = \Phi - \pi/2$ .

Furthermore we have, on equating the representations of  $x$  and  $y$  in (B 7) and (B 14),

$$\frac{\partial \mathcal{P}}{\partial \mathcal{R}} = \frac{1}{\mathcal{R}^n} \frac{\partial \hat{\Psi}}{\partial \Phi}, \quad \frac{\partial \mathcal{P}}{\partial \Phi} = -\frac{1}{n\mathcal{R}^{n-2}} \frac{\partial \hat{\Psi}}{\partial \mathcal{R}}. \tag{B 15}$$

Now since

$$\hat{\Psi} = -e^{-n\beta} \left( nr \frac{\partial \beta}{\partial r} + 1 \right), \quad \mathcal{R}^n = ne^{-n\beta} |\nabla \beta|,$$

we have in the limit  $n \rightarrow +\infty$  that

$$\frac{\hat{\Psi}}{\mathcal{R}^n} = -r \frac{\beta_r}{|\nabla \beta|}, \tag{B 16}$$

which motivates the introduction of

$$B = r \frac{\beta_r}{|\nabla \beta|}, \tag{B 17}$$

as the dependent variable, in transform space, that corresponds to  $\beta$ . From (B 15) we then have, in the limit, that

$$\frac{\partial P}{\partial \mathcal{R}} = \frac{\partial B}{\partial \Phi}, \quad \frac{\partial P}{\partial \Phi} = -\mathcal{R}B,$$

from which we recover (B 12) together with

$$\frac{\partial}{\partial \mathcal{R}}(\mathcal{R}B) + \frac{\partial^2 B}{\partial \Phi^2} = 0. \tag{B 18}$$

**B.2 Alternative derivations of the heat equation from (B 3)**

For flow by the reciprocal of the mean curvature  $\kappa$ ,

$$q_N = -\frac{1}{\kappa},$$

a level set of  $F(x, t)$  evolves according to

$$\frac{\partial F}{\partial t} = -\frac{|\nabla F|}{\nabla \cdot (\nabla F / |\nabla F|)}.$$

Setting  $F = t - \beta(x, y)$  yields (B 3), whilst writing  $F = y - f(x, t)$  gives

$$\frac{\partial f}{\partial t} = -\frac{(1 + f_x^2)^2}{f_{xx}}, \tag{B 19}$$

which can also be derived from (B 3) by the partial hodograph transformation

$$t = \beta, \quad f = y.$$

Note that, here  $t$  is an artificial time-like variable (not time itself as in the rest of the paper) and that partial derivatives of  $\beta$  transform according to

$$\frac{\partial \beta}{\partial y} = \left(\frac{\partial f}{\partial t}\right)^{-1}, \quad \frac{\partial \beta}{\partial x} = -\frac{\partial f}{\partial x} \left(\frac{\partial f}{\partial t}\right)^{-1}. \tag{B 20}$$

Now, (B 19) belongs to a class of PDE identified in [24] as being linearisable by the Legendre transformation

$$\hat{f} = x \frac{\partial f}{\partial x} - f, \quad \hat{x} = \frac{\partial f}{\partial x}, \quad t' = t, \tag{B 21}$$

with inverse

$$f = \hat{x} \frac{\partial \hat{f}}{\partial \hat{x}} - \hat{f}, \quad x = \frac{\partial \hat{f}}{\partial \hat{x}}, \quad t = t'. \tag{B 22}$$

This transformation of (B 19) yields

$$\frac{\partial \hat{f}}{\partial t'} = (1 + \hat{x}^2)^2 \frac{\partial^2 \hat{f}}{\partial \hat{x}^2}; \tag{B 23}$$

indeed, the general class noted in [24] as linearisable in this fashion can be given an interfacial-dynamics interpretation as anisotropic flow by inverse curvature

$$V = \frac{\Theta(\theta)}{\kappa}, \quad \frac{\partial f}{\partial t} = -\frac{\Theta(\tan^{-1} f_x)(1 + f_x^2)^2}{f_{xx}}. \tag{B 24}$$

From (B 21) we have  $\hat{x} = \tan \theta$  (where  $\theta$  is the angle the tangent to the curve  $y = f(x, t)$  makes with the  $x$ -axis). Setting  $\hat{f}(\hat{x}, t) = \sec \theta \hat{g}(\theta, t)$  then transforms (B 23) to

$$\frac{\partial \hat{g}}{\partial t} = \frac{\partial^2 \hat{g}}{\partial \theta^2} + \hat{g}. \tag{B 25}$$

Moreover, it can readily be shown (using  $f_t = -\hat{f}_t, f_{xx} = 1/\hat{f}_{\hat{x}\hat{x}}$ ) that

$$\frac{1}{\kappa} = \frac{\partial^2 \hat{g}}{\partial \theta^2} + \hat{g}, \quad V = \frac{\partial \hat{g}}{\partial t},$$

and that the radius of curvature accordingly satisfies a linear equation

$$\frac{\partial}{\partial t} \left(\frac{1}{\kappa}\right) = \frac{\partial^2}{\partial \theta^2} \left(\frac{1}{\kappa}\right) + \frac{1}{\kappa}. \tag{B 26}$$

Since  $1/\kappa = \partial s/\partial \theta$ , the arc length  $s(\theta, t)$  does likewise. Equation (B 26) is a particular case of the plane-curve evolution equation

$$\frac{\partial}{\partial t} \left(\frac{1}{\kappa}\right) = \frac{\partial^2 V}{\partial \theta^2} + V,$$

(see [19], for example), from which it is again clear that (B 24) maps to a linear PDE. Finally in this context, we note that (B 1), (B 5) and (B 9) imply

$$\cos \Phi = \frac{1}{|\nabla\beta|} \frac{\partial\beta}{\partial y}, \quad \sin \Phi = \frac{1}{|\nabla\beta|} \frac{\partial\beta}{\partial x},$$

so by (B 20), (B 21)

$$\hat{X} = \tan \Phi,$$

i.e. the angle  $\theta$  just introduced is identical to the polar angle  $\Phi$  in the Legendre plane. It then follows that

$$\hat{g} = \cos \theta \hat{f} = \cos \theta \left( x \frac{\partial f}{\partial x} - f \right) = -\frac{1}{|\nabla\beta|} \left( x \frac{\partial\beta}{\partial x} + y \frac{\partial\beta}{\partial y} \right) = -B,$$

and the equivalence between (B 18) and (B 25) is then immediate. We have in the above outlined a number of distinct, but equivalent, frameworks through which (B 2) can be transformed to a linear PDE equivalent to the heat equation. The reasons for doing so are twofold, firstly to bring together transformations that have previously been separately identified in a number of distinct contexts and, secondly, because the most convenient representation to adopt may depend on the boundary value problem in question. For completeness, we conclude by outlining two further restatements.

### B.3 Hodograph transformation

In [3], Aronsson reformulates (B 4) by a hodograph transformation that corresponds to interchanging the roles of  $(p, \beta)$  and  $(x, y)$ . We first generalise this to (2.4) to make explicit the nature of the resulting  $n \rightarrow +\infty$  limit, with  $(p, \psi)$  as the new independent variables. Thus, by using the chain rule on the expressions

$$\begin{aligned} \frac{\partial}{\partial p} p(x(p, \psi), y(p, \psi)) &= 1, & \frac{\partial}{\partial \psi} p(x(p, \psi), y(p, \psi)) &= 0, \\ \frac{\partial}{\partial \psi} \psi(x(p, \psi), y(p, \psi)) &= 1, & \frac{\partial}{\partial p} \psi(x(p, \psi), y(p, \psi)) &= 0, \end{aligned}$$

and inverting these we obtain the following expressions:

$$\frac{\partial p}{\partial x} = \mathfrak{J} \frac{\partial y}{\partial \psi}, \quad \frac{\partial p}{\partial y} = -\mathfrak{J} \frac{\partial x}{\partial \psi}, \quad \frac{\partial \psi}{\partial x} = -\mathfrak{J} \frac{\partial y}{\partial p}, \quad \frac{\partial \psi}{\partial y} = \mathfrak{J} \frac{\partial x}{\partial p},$$

where

$$\mathfrak{J} \equiv \left( \frac{\partial x}{\partial p} \frac{\partial y}{\partial \psi} - \frac{\partial x}{\partial \psi} \frac{\partial y}{\partial p} \right)^{-1} = \frac{\partial p}{\partial x} \frac{\partial \psi}{\partial y} - \frac{\partial p}{\partial y} \frac{\partial \psi}{\partial x}.$$

It follows that

$$\mathfrak{J} = -|\nabla p|^{n+1} = -|\nabla \psi|^{1+1/n},$$

these being the integrands in the variational principles from which (1.1) can be deduced. In consequence  $x(p, \psi)$  and  $y(p, \psi)$  satisfy the system

$$\frac{\partial x}{\partial p} = - \left( \left( \frac{\partial x}{\partial \psi} \right)^2 + \left( \frac{\partial y}{\partial \psi} \right)^2 \right)^{-\frac{n-1}{2n}} \frac{\partial y}{\partial \psi}, \quad \frac{\partial y}{\partial p} = \left( \left( \frac{\partial x}{\partial \psi} \right)^2 + \left( \frac{\partial y}{\partial \psi} \right)^2 \right)^{-\frac{n-1}{2n}} \frac{\partial x}{\partial \psi},$$

$$\text{with} \quad \left( \frac{\partial x}{\partial p} \right)^2 + \left( \frac{\partial y}{\partial p} \right)^2 = \left( \left( \frac{\partial x}{\partial \psi} \right)^2 + \left( \frac{\partial y}{\partial \psi} \right)^2 \right)^{1/n}.$$

Introducing  $\beta$  (as above) and letting  $n \rightarrow +\infty$  yields

$$\frac{\partial x}{\partial p} \frac{\partial x}{\partial \beta} + \frac{\partial y}{\partial p} \frac{\partial y}{\partial \beta} = 0, \quad \left( \frac{\partial x}{\partial p} \right)^2 + \left( \frac{\partial y}{\partial p} \right)^2 = e^{2\beta},$$

a degenerate limit consistent with the results of [3].

### B.4 ‘Characteristic’ approach

Our last approach (which is not restricted to the two-dimensional case and in which the notation differs from that above) builds upon that in [17] which considers ‘characteristic’ curves  $\dot{\mathbf{x}} = \nabla p$  for (B4). Given that the application here is to fluid flow, it is more natural physically to set  $\dot{\mathbf{x}} = -|\nabla p|^{n-1} \nabla p$  in considering (1.1), but in any case we generalise to

$$\frac{d}{dt} \mathbf{x}(\mathbf{X}, t) = -M(|\nabla p(\mathbf{x})|) \nabla p(\mathbf{x}) \quad \text{at } t = 0 \quad \mathbf{x} = \mathbf{X}, \tag{B 27}$$

viewing this as a relationship between ‘Lagrangian’ and ‘Eulerian’ coordinates ( $t$  is again not the true time; as the notation on the right-hand side of (B 27) implies, we are here investigating the elliptic problem (1.1) frozen in time). From (B 27) it follows that

$$\frac{d}{dt} p(\mathbf{x}) = -M(|\nabla p|) |\nabla p|^2, \quad \frac{d}{dt} |\nabla p(\mathbf{x})| = -M(|\nabla p|) \nabla p \cdot \nabla |\nabla p|, \tag{B 28}$$

at fixed  $\mathbf{X}$  and hence that

$$\frac{d^2}{dt^2} p(\mathbf{x}) = \left\{ M(R) \frac{d}{dR} (R^2 M(R)) \right\} \Big|_{R=|\nabla p|} \nabla p \cdot \nabla |\nabla p|, \tag{B 29}$$

The infinity-Laplace operator thus arises naturally here and when (B 4) holds we have

$$|\nabla_{\mathbf{x}} p(\mathbf{x})| = |\nabla_{\mathbf{X}} p(\mathbf{X})|, \quad p(\mathbf{x}) = p(\mathbf{X}) - M(|\nabla p|) |\nabla p|^2 t. \tag{B 30}$$

Since (B 4) and (B 27) imply that the flow is tangential to the level sets of  $|\nabla p|$  (and level sets of  $p$ , the isobars, are steepest-descent directions of the speed  $|\nabla p|$  and vice versa), the first of (B 28) is immediate. The more general case is worth pursuing, however, not least for the insight it gives into region V. Now defining  $J = \det(\partial x_i / \partial X_j)$  (a quantity familiar in continuum mechanics), by standard arguments we have

$$\frac{dJ}{dt} = -\nabla \cdot (M(|\nabla p|) \nabla p) J. \tag{B 31}$$

Considering in the first instance the more general equation

$$\nabla \cdot (D(|\nabla p|)\nabla p) = 0. \quad (\text{B } 32)$$

It follows from (B 28) and (B 31) that

$$\frac{d}{dR} \left( \log \left( \frac{M}{D} \right) \right) \Big|_{R=|\nabla p|} \frac{d}{dt} |\nabla p| = \frac{1}{J} \frac{dJ}{dt},$$

so that  $J$  takes the separable form

$$J = \frac{M(|\nabla_{\mathbf{x}} p(\mathbf{x})|)D(|\nabla_{\mathbf{X}} p(\mathbf{X})|)}{D(|\nabla_{\mathbf{x}} p(\mathbf{x})|)M(|\nabla_{\mathbf{X}} p(\mathbf{X})|)}.$$

Setting  $M = D$  gives the usual incompressibility result  $J \equiv 1$ ; for our purposes, a more interesting case for  $D(R) = R^{n-1}$  is where we set  $M(R) = R^\gamma$  to give

$$J = \left( \frac{|\nabla_{\mathbf{X}} p(\mathbf{X})|}{|\nabla_{\mathbf{x}} p(\mathbf{x})|} \right)^{n-1-\gamma}; \quad (\text{B } 33)$$

this implies the first of (B 30) in the limit  $n \rightarrow +\infty$  and its strong dependence on  $n$  has bearing on the understanding of region V.

Our final (cursory) remark here was triggered by the description in [17] of how (B 4) can be regarded as being in divergence form (that (B 4) is not, unlike (1.1), obviously of such a form is a little mysterious given that the former is a limit case of the latter). Applying the divergence theorem to the second of (1.1) a bounded domain  $\Omega$  in the absence of a source<sup>2</sup> gives

$$\oint_{\partial\Omega} |\nabla p|^{n-1} \frac{\partial p}{\partial N} dS = 0, \quad (\text{B } 34)$$

so that the integral will be dominated, in the limit  $n \rightarrow +\infty$ , by the points on the boundary  $\partial\Omega$  at which  $|\nabla p|$  is maximal, whereby the tangential derivatives of  $|\nabla p|$  will be zero (in the presence of a source, this dominance is associated with the yielded region), (B 34) then requires that the normal derivative of  $p$  also vanish at such points, consistent with the orthogonality of  $\nabla p$  and  $\nabla|\nabla p|$  implied by (B 4). In this naive interpretation, in the limit that the surface integral (B 34) collapses to a result at individual points on the surface, this being associated with (B 4) losing the obvious divergence form present in (1.1).

## References

- [1] ALEXANDROU, A. N. & ENTOV, V. (1997) On the steady-state advancement of fingers and bubbles in a Hele-Shaw cell filled by a non-Newtonian fluid. *Euro. J. Appl. Math.* **8**, 73–87.
- [2] ARONSSON, G. (1996) On  $p$ -harmonic functions, convex duality and an asymptotic formula for injection moulding. *Euro. J. Appl. Math.* **8**, 417–437.
- [3] ARONSSON, G. (1968) On the partial differential equation  $u_x^2 u_{xx} + 2u_x u_y u_{xy} + u_y^2 u_{yy} = 0$ . *Arkiv für Mat.* **7**, 395–425.

<sup>2</sup> We have in the above been notationally sloppy in dealing with the source.

- [4] ARONSSON, G. (2003) Five geometric principles of injection moulding. *Intern. Polymer Proc.* **18**, 91–94.
- [5] ARONSSON, G. & EVANS, L. C. (2002) An asymptotic model for compression molding. *Indiana Univ. Math. J.* **51**, 1–36.
- [6] ARONSSON, G. & JANFALK, U. (1992) On Hele-Shaw flows of power law fluids. *Euro. J. Appl. Math.* **3**, 343–366.
- [7] ATKINSON, C. & CHAMPION, C. R. (1984) Some boundary-value-problems for the equation  $\nabla \cdot (|\nabla\phi|^N \nabla\phi) = 0$ . *Q. J. Mech. Appl. Math.* **37**, 401–419.
- [8] BEN AMAR, M. & CORVEIRA POIRE, E. (1998) Finger behaviour of shear thinning fluid in a Hele-Shaw cell. *Phys. Rev. Lett.* **81**, 2048–2051.
- [9] BEN AMAR, M. & CORVEIRA POIRE, E. (1999) Pushing a non-Newtonian fluid in a Hele-Shaw cell: From fingers to needles. *Phys. Fluids* **11**, 1757–1767.
- [10] BERGWALL, A. (2002) A geometric evolution problem. *Quart. Appl. Math.* **50**, 37–73.
- [11] BREWSTER, M. A., CHAPMAN, S. J., FITT, A. D. & PLEASE, C. P. (1995) Asymptotics of slow flow of very small exponent shear thinning fluids in a wedge. *Euro. J. Appl. Math.* **6**, 559–571.
- [12] CENICEROS, H. D., HOU, T. Y. & SI, H. (1999) Numerical study of Hele-Shaw flow with suction. *Phys. Fluids* **11**, 2471–2486.
- [13] CHAPMAN, S. J., FITT, A. D. & PLEASE, C. P. (1997) Extrusion of power law shear thinning fluids with small exponent. *Int. J. Non-Linear Mech.* **32**, 187–199.
- [14] CUMMINGS, L. J. & KING, J. R. (2004) Hele-Shaw flow with a point sink: Generic solution breakdown. *Euro. J. Appl. Math.* **15**, 1–37.
- [15] DRUCKER, D. & WILLIAMS, S. A. (2009) A note on Aronsson's equation. *Rocky Mt. J. Math.* **39**, 1859–1869.
- [16] EVANS, L. C. (1991) The 1-Laplacian, the  $\infty$ -Laplacian and differential games. URL: <http://math.berkeley.edu/~evans/brezis.pdf>
- [17] EVANS, L. C. & YU, Y. (2005) Various properties of solutions of the Infinity-Laplacian equation. *Comm. Partial Differ. Equ.* **30**, 1401–1428.
- [18] GALIN, L. A. (1945) Unsteady filtration with a free surface. *Dokl. Akad. Nauk SSSR* **7**, 250–253 (in Russian).
- [19] GURTIN, M. E. (1993) *Thermomechanics of Evolving Phase Boundaries in the Plane*, OUP, Oxford.
- [20] HOWISON, S. D. (1992) Complex variable methods in Hele-Shaw moving boundary problems. *Euro. J. Appl. Math.* **3**, 209–224.
- [21] HOWISON, S. D., LACEY, A. A. & OCKENDON, J. R. (1988) Hele-Shaw Free boundary problems with suction. *Quart. J. Mech. Appl. Math.* **41**, 183–193.
- [22] HOWISON, S. D., MORGAN, J. D. & OCKENDON, J. R. (1997) A class of codimension two free boundary problems. *SIAM Rev.* **39**, 221–253.
- [23] KELLY, E. D. & HINCH, E. J. (1997) Numerical simulations of sink flow in the Hele-Shaw cell with small surface tension. *Euro. J. Appl. Math.* **8**, 553–550.
- [24] KING, J. R. (1990) Some non-local transformations between nonlinear diffusion equations. *J. Phys. A* **23**, 5441–5464.
- [25] KING, J. R. (1995) Development of singularities in some moving boundary value problems. *Euro. J. Appl. Math.* **6**, 491–507.
- [26] MULLINS, W. W. (1956) Two-dimensional motion of idealised grain boundaries. *J. Appl. Phys.* **27**, 900–904.
- [27] MOSER, R. (2007) The inverse mean curvature flow and p-harmonic functions. *J. Eur. Math. Soc.* **9**, 77–83.
- [28] OCKENDON, J. R. & HOWISON, S. D. (2002) Kochina and Hele-Shaw in modern mathematics, natural science and industry. *J. Appl. Math. Mech.* **66**, 505–512.
- [29] PISCOTTI, F., BOLDIZAR, A., RIGHDAL, M. & ARONSSON, G. (2002) Evaluation of a model describing the advancing flow front in injection moulding. *Intern. Polymer Proc.* **17**, 133–145.

- [30] POLUBARINOVA-KOCHINA, P. YA. (1945) On the motion of the oil contour. *Dokl. Akad. Nauk SSSR* **47**, 254–257 (in Russian).
- [31] RICHARDSON, S. (1981) Some Hele Shaw flows with time-dependent free boundaries. *J. Fluid Mech.* **102**, 263–278.
- [32] RICHARDSON, G. & KING, J. R. (2007) The Saffman-Taylor problem for an extremely shear-thinning fluid. *Quart. J. Mech. Appl. Math.* **60**, 139–160.
- [33] RICHARDSON, G. & KING, J. R. (2002) Motion by curvature of a three-dimensional filament: Similarity solutions. *Interfaces Free Boundaries* **4**, 395–421.
- [34] RICHARDSON, G. & KING, J. R. (2002) The evolution of space curves by curvature and torsion. *J. Phys. A: Math. Gen.* **35**, 9857–9879.
- [35] SAPIRO, G. & TANNENBAUM, A. (1992) Affine invariant scale space. *Int. J. Comput. Vis.* **11**, 25–44.
- [36] SMOCZYK, K. (2005) A representation formula for the inverse harmonic mean curvature flow. *Elemente der Math.* **60**, 57–65.
- [37] TANVEER, S. (2000) Surprises in viscous fingering. *J. Fluid Mech.* **409**, 273–308.